Munc18c phosphorylation by the insulin receptor links cell signaling directly to SNARE exocytosis

Jenna L. Jewell,[1] Eunjin Oh,[2] Latha Ramalingam,[1] Michael A. Kalwat,[1] Vincent S. Tagliabracci,[1] Lixuan Tackett,[3] Jeffrey S. Elmendorf,[1,3] and Debbie C. Thurmond[1,2,3]

[1]Department of Biochemistry and Molecular Biology, [2]Department of Pediatrics, and [3]Department of Cellular and Integrative Physiology, Indiana University School of Medicine, Indianapolis, IN 46202

How the Sec1/Munc18–syntaxin complex might transition to form the SNARE core complex remains unclear. Toward this, Munc18c tyrosine phosphorylation has been correlated with its dissociation from syntaxin 4. Using 3T3-L1 adipocytes subjected to small interfering ribonucleic acid reduction of Munc18c as a model of impaired insulin-stimulated GLUT4 vesicle exocytosis, we found that coordinate expression of Munc18c–wild type or select phosphomimetic Munc18c mutants, but not phosphodefective mutants, restored GLUT4 vesicle exocytosis, suggesting a requirement for Munc18c tyrosine phosphorylation at Tyr219 and Tyr521. Surprisingly, the insulin receptor (IR) tyrosine kinase was found to target Munc18c at Tyr521 in vitro, rapidly binding and phosphorylating endogenous Munc18c within adipocytes and skeletal muscle. IR, but not phosphatidylinositol 3-kinase, activation was required. Altogether, we identify IR as the first known tyrosine kinase for Munc18c as part of a new insulin-signaling step in GLUT4 vesicle exocytosis, exemplifying a new model for the coordination of SNARE assembly and vesicle mobilization events in response to a single extracellular stimulus.

Introduction

Sec1/Munc18 (SM) proteins are essential regulators of SNARE protein–mediated vesicle budding/fusion events, initially identified as high affinity binding partners for t-SNARE syntaxin proteins and, more recently, in a binding mode with the SNARE core complex. SM proteins are conserved in *Saccharomyces cerevisiae* (Sec1), *Caenorhabditis elegans* (Unc18), *Drosophila melanogaster* (ROP), and mammalian systems (Munc18). Mammalian cells express three plasma membrane–localized isoforms, which regulate vesicle exocytosis, commonly referred to as Munc18-1/nSec1, Munc18b, and Munc18c, which share >50% sequence similarity. Among the three plasma membrane isoforms, Munc18-1 expression is restricted to neuronal cells and pancreatic islet β cells, whereas Munc18b and Munc18c are ubiquitously expressed (Tellam et al., 1995; Zhang et al., 2000). Similarly, numerous syntaxin isoforms exist and pair with their cognate SM proteins in an isoform-specific manner: syntaxin isoforms 1–3, but not 4, associate with Munc18-1 and Munc18b, whereas Munc18c pairs exclusively with syntaxin 4 (Tellam et al., 1995, 1997). Despite sharing a similar three-dimensional crystallographic crescent shape (Misura et al., 2000; Hu et al., 2007), the specifiers of Munc18-1 and Munc18c differentially pairing with syntaxin 1 versus syntaxin 4, respectively, remain elusive.

Studies of the neuronal Munc18-1 isoform show its ability to engage in multiple modes of interactions with syntaxin 1 and the SNARE complex. The newest mode supports a facilitating role for Munc18-1 in the fusion step of the exocytosis process (Shen et al., 2007; Südhof and Rothman, 2009). Specifically, fusion occurs once the v-SNARE protein present on the vesicle membrane associates with the two t-SNARE proteins present on the plasma membrane to form a bundle composed of four α helices, or a "SNAREpin" (Weber et al., 1998). Additional binding of Munc18-1 to this bundle is proposed as the activating factor to promote fusion of the vesicle with the plasma membrane

J.L Jewell and E. Oh contributed equally to this paper.

Correspondence to Debbie C. Thurmond: dthurmon@iupui.edu

J.L. Jewell's and V.S. Tagliabracci's present address is Dept. of Pharmacology, University of California, San Diego, La Jolla, CA 92093.

Abbreviations used in this paper: DLK, dual leucine zipper kinase; HNMPA-$(AM)_3$, hydroxy-2-napthalenylmethylphosphoric acid tris-acetoxy-methyl ester; IR, insulin receptor; IRS, IR substrate; PI3K, phosphatidylinositol 3-kinase; pV, pervanadate; PVDF, polyvinylidene fluoride; shRNA, small hairpin RNA; siCon, control siRNA; SM, Sec1/Munc18; WT, wild type.

The Rockefeller University Press $30.00
J. Cell Biol. Vol. 193 No. 1 185–199
www.jcb.org/cgi/doi/10.1083/jcb.201007176

(Shen et al., 2010). In its restrictive/inhibitory mode, Munc18-1 can associate with a "closed" form of syntaxin 1, presumably preventing its participation in SNARE core complexes (Dulubova et al., 1999; Misura et al., 2000). Complicating the delineation of a clear model for how transitions between modes might occur, Munc18-1 overexpression studies have shown both enhancement and inhibition of exocytosis (Schulze et al., 1994; Wu et al., 1998; Toonen et al., 2006; Shen et al., 2007, 2010; Südhof and Rothman, 2009).

In contrast, overexpression of the Munc18c isoform consistently inhibits vesicle exocytosis (Tamori et al., 1998; Thurmond et al., 1998; Khan et al., 2001; Spurlin et al., 2003), supporting the concept of its inhibitory mode. However, additional Munc18c gene deletion studies show it to be required for slow exocytosis events, such as second-phase insulin release from islets and insulin-stimulated GLUT4 vesicle accumulation in skeletal muscle surface membranes (Oh et al., 2005; Oh and Thurmond, 2009), both of which involve the stimulus-induced mobilization, tethering/docking, and fusion of vesicles housed in deeper and nonreadily releasable cell storage compartments. Specifically, Munc18c is required for stimulus-induced syntaxin 4–based exocytosis events, suggesting that Munc18c must somehow release syntaxin 4 for docking/fusion events to proceed. Notably, Munc18c has been shown to undergo stimulus-induced tyrosine phosphorylation at two discrete motifs to dissociate from syntaxin 4, at Tyr219 in islet β cells and Tyr521 in 3T3-L1 adipocytes (Oh and Thurmond, 2006; Schmelzle et al., 2006; Umahara et al., 2008). However, it remains untested as to whether the tyrosine phosphorylation of Munc18c is functionally essential for syntaxin 4–mediated exocytosis.

The 3T3-L1 adipocyte model of GLUT4 vesicle exocytosis may be an ideal system to test the hypothesis that tyrosine phosphorylation of Munc18c results in syntaxin 4 release and function in exocytosis. Munc18c appears to be the sole functional plasma membrane–localized SM protein, with Munc18b shown to be functionally inert (Tamori et al., 1998; Thurmond et al., 1998; Khan et al., 2001). Unlike the islet β cell, which expresses and utilizes multiple Munc18–syntaxin complexes for multiple phases of insulin release, 3T3-L1 adipocytes use only the Munc18c–syntaxin 4 pair for the monophasic process of insulin-stimulated GLUT4 vesicle exocytosis (Timmers et al., 1996; Olson et al., 1997; Tamori et al., 1998; Thurmond et al., 1998). This is similarly representative of skeletal muscle function in vivo because heterozygous knockout of either syntaxin 4 or Munc18c genes in mice results in the attenuation of insulin-stimulated glucose uptake correlated with the disruption of whole-body glucose homeostasis, insulin resistance, and increased susceptibility to the development of type 2 diabetes, which is caused, in large part, by the absence of skeletal muscle GLUT4 vesicle exocytosis in response to insulin (Yang et al., 2001; Oh et al., 2005). Strikingly, reduced protein and/or mRNA levels of Munc18c and syntaxin 4 are reported in obese and type 2 diabetic human subjects as well as rodent obese and diabetic models (Yechoor et al., 2004; Bergman et al., 2008; Keller et al., 2008).

Emerging evidence suggests that insulin likely regulates various aspects of GLUT4 exocytosis via multiple signaling pathways, many of which have been characterized in the 3T3-L1 adipocyte system. In the adipocyte, >95% of preformed GLUT4 vesicles are absent from the plasma membrane under resting conditions, requiring insulin signaling for mobilization and vesicle fusion to achieve GLUT4 deposition into the plasma membrane. One main insulin transduction pathway entails a phosphatidylinositol 3-kinase (PI3K) signal involving the upstream insulin receptor (IR) and IR substrate (IRS) activators and the downstream Akt2 target enzyme (Huang and Czech, 2007; Gonzalez and McGraw, 2009; Klip, 2009). An accessory signaling pathway that targets and/or tethers the activated GLUT4 vesicle at and/or near the plasma membrane has also been previously described (Inoue et al., 2003; Chen et al., 2007). Moreover, a postdocking signal that primes the GLUT4 vesicle at the plasma membrane for fusion competence has been previously suggested (Gonzalez and McGraw, 2006; Bai et al., 2007). Concurrent with these signaling pathways, the plasma membrane–localized t-SNARE exocytosis machinery apparently must undergo a regulated assembly for the incoming vesicles (Takahashi et al., 2010). Whether this represents another GLUT4 regulatory signaling pathway of insulin action remains unknown.

Taking advantage of this model system in the present study, we identify IR as the first known tyrosine kinase for Munc18c and provide evidence to suggest a requirement for the tyrosine phosphorylation of Munc18c in normal GLUT4 vesicle exocytosis. Unlike wild-type (WT) Munc18c and phosphomimetic Munc18c mutants, phosphorylation-defective mutants failed to show insulin-stimulated release of syntaxin 4 from Munc18c. These observations may provide insight into how the SM proteins interacting in the inhibitory mode can release their cognate syntaxin in a stimulus-dependent manner to facilitate vesicle fusion. From a broader cell biology perspective, the ubiquitous Munc18c and syntaxin 4 machinery might be posttranslationally tailored to suit the stimulus-specific response of a given cell type, effectively functioning in a tissue-specific manner, obviating the need for each cell-specific exocytosis event to use novel SNARE and SM proteins.

Results

IR binds to and tyrosine phosphorylates Munc18c

Skeletal muscle is responsible for ∼80% of glucose uptake and clearance through GLUT4 exocytosis, responding to insulin stimulation in a manner similar to that of adipocytes (Foster and Klip, 2000). Although rapid insulin-stimulated tyrosine phosphorylation of Munc18c has been observed in 3T3-L1 adipocytes (Oh and Thurmond, 2006; Schmelzle et al., 2006; Umahara et al., 2008), it has yet to be reported for skeletal muscle. To address this, we compared the magnitude of tyrosine phosphorylation of Munc18c between these insulin-responsive cell types. Although unstimulated adipocytes contained a low but detectable level of tyrosine-phosphorylated Munc18c, Munc18c tyrosine phosphorylation levels rose approximately twofold to peak at 5 min of insulin stimulation (Fig. 1 A). Similarly, the level of Munc18c tyrosine phosphorylation in hind-limb muscle extracts from mice injected intraperitoneally with insulin increased

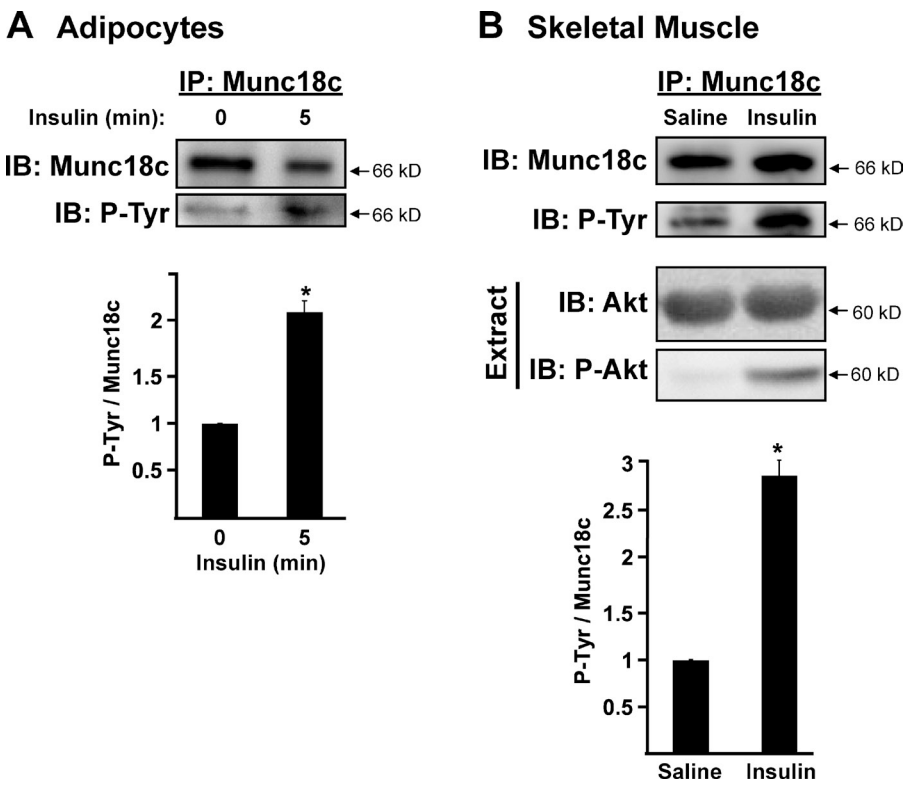

Figure 1. **Insulin stimulation increases Munc18c tyrosine phosphorylation.** (A) Munc18c was immunoprecipitated (IP) from cleared detergent cell lysates prepared from fully differentiated 3T3-L1 adipocytes that were incubated in serum-free medium for 2 h and then stimulated with 100 nM insulin for 5 min. Proteins were resolved by 10% SDS-PAGE, immunoblotted (IB) for Munc18c, stripped, and reblotted for detection of tyrosine-phosphorylated (P-Tyr) Munc18c using the 4G10 antibody. Data were collected from four independent experiments quantified as the ratio of tyrosine-phosphorylated Munc18c/total Munc18c precipitated and normalized to basal set = 1.0; *, $P < 0.05$ versus basal. (B) Munc18c was immunoprecipitated from hind-limb muscle extracts prepared from mice injected with vehicle (saline) or insulin (10 U/kg of body weight) for 5 min as described in Materials and methods. Proteins were resolved by 10% SDS-PAGE, immunoblotted for Munc18c, stripped, and reprobed for detection of tyrosine-phosphorylated Munc18c using the 4G10 antibody. Insulin action in the starting lysates was validated by detection of threonine 308–phosphorylated Akt (P-Akt) in extracts, which was relative to total Akt present on the same blot (stripped and reprobed). Data were quantified from 12 extracts (6 mice for each treatment) as the ratio of tyrosine-phosphorylated Munc18c/total Munc18c and normalized to saline controls = 1.0; *, $P < 0.05$ versus saline-injected controls. Data represent means ± SEM.

nearly threefold within 5 min compared with saline-injected muscle extracts (Fig. 1 B). The action of insulin was validated by the detection of phospho-Akt selectively in the insulin-stimulated muscle extracts. These data suggested that the rapid insulin stimulation of Munc18c tyrosine phosphorylation might be a conserved mechanism used by divergent cell types that share in common GLUT4 vesicle exocytosis.

To identify the Munc18c kinase, inspection of the Munc18c amino acid sequence by the ExPASy Proteomics Server (NetPhosk 1.0 Server) and Group-based Prediction System (Xue et al., 2008) was used, revealing potential IR tyrosine phosphorylation consensus sites (underlined) at Tyr219 (EKKLEDY<u>Y</u>KIDEKGL) and Tyr521 (RQKPRTN<u>Y</u>LELDRKN); both sites corresponded to those previously identified biochemically as important for Munc18c–syntaxin 4 binding (Oh and Thurmond, 2006; Schmelzle et al., 2006; Umahara et al., 2008). To test this prediction, insulin-stimulated adipocyte and muscle extracts were subjected to anti-Munc18c immunoprecipitation and coprecipitation of the IR assessed. Compared with only slight coprecipitation under basal conditions, insulin stimulated approximately twofold more IR coprecipitation in both 3T3-L1 adipocyte lysates (Fig. 2 A) and muscle extracts (Fig. 2 B) versus unstimulated controls. The action of IR within these extracts was confirmed by the demonstration of a similar increase in IR coimmunoprecipitation with its well-known substrate IRS-1 (Fig. S1 A). Interestingly, Munc18c and IRS-1 failed to coprecipitate (Fig. S1, A and B), suggesting that IR–Munc18c complexes may be mutually exclusive of IR–IRS-1 complexes. Our data expand upon this by suggesting that IR–Munc18c function is a required but distinct step from that of IR/IRS/PI3K signaling in the process of GLUT4 vesicle translocation.

To establish whether the binding of IR to Munc18c and the tyrosine phosphorylation of Munc18c were linked, we used pervanadate (pV) to inhibit the protein tyrosine phosphatase activity in lieu of insulin stimulation and reevaluated these binding and phosphorylation events. Indeed, in lysates prepared from 3T3-L1 adipocytes treated with pV, Munc18c coimmunoprecipitated IR (Fig. 3 A, *i*). Moreover, cells treated with pV contained significantly more tyrosine-phosphorylated Munc18c compared with untreated cells (Fig. 3 A, *ii*). Reciprocal coimmunoprecipitation experiments using the anti-IR antibody confirmed these results (Fig. 3 B) and further revealed the absence of syntaxin 4 association with the pV-stimulated IR–Munc18c complex. Because syntaxin 4 failed to coprecipitate with IR also under untreated conditions, which could be otherwise attributed to steric hindrance, the reciprocal coimmunoprecipitation was performed using the anti–syntaxin 4 antibody. However, syntaxin 4 failed to coprecipitate IR (Fig. 3 C). Importantly, pV treatment resulted in an ∼60% decrease in Munc18c–syntaxin 4 association; insulin stimulation for 5 min in adipocytes was previously shown to exert a similar effect (Oh and Thurmond, 2006). These data suggested possible linkages between insulin-stimulated IR–Munc18c binding, tyrosine-specific phosphorylation, and Munc18c–syntaxin 4 dissociation events.

Munc18c tyrosine phosphorylation requires IR kinase activity in a pathway independent of PI3K activation

To more specifically determine whether IR kinase activity was required for Munc18c phosphorylation, the IR-specific inhibitor

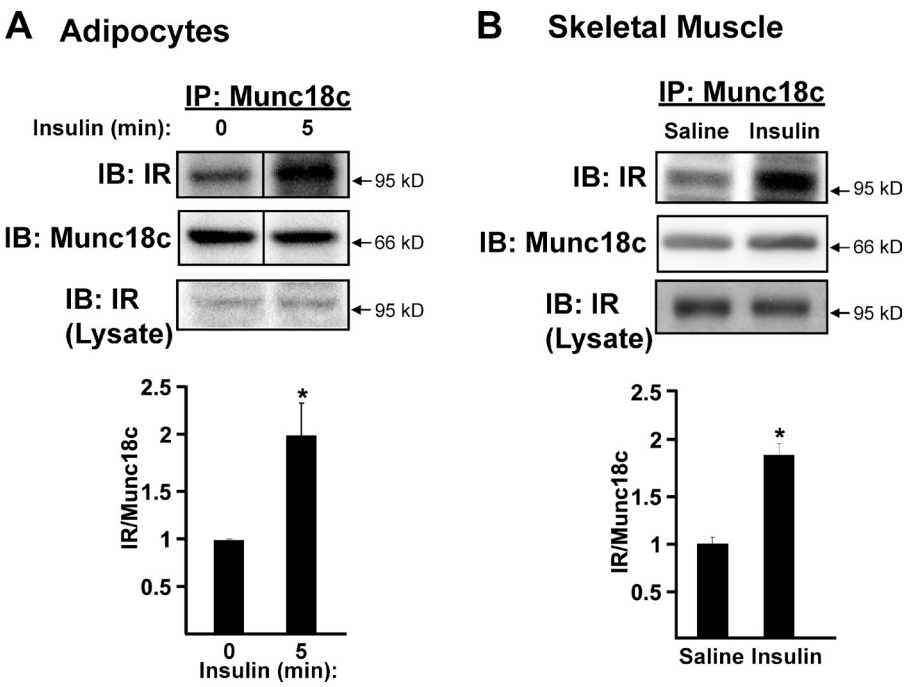

Figure 2. **Insulin stimulates the association of IR with Munc18c.** (A) Munc18c was immunoprecipitated (IP) from cleared detergent lysates prepared from fully differentiated 3T3-L1 adipocytes that were incubated in serum-free medium for 2 h and then stimulated with 100 nM insulin for 5 min. Proteins were resolved by 10% SDS-PAGE and immunoblotted (IB) with anti-Munc18c and anti–insulin receptor (IR) antibodies. Data are from three independent sets of lysates quantified as the ratio of IR–Munc18c, with each set normalized to basal = 1.0; *, $P < 0.05$. (B) Munc18c was immunoprecipitated from hind-limb muscle extracts prepared from mice injected with vehicle (saline) or insulin (10 U/kg of body weight) for 5 min and processed for analysis as described in Fig. 1 B; *, $P < 0.05$ versus saline-injected controls. Equivalent IR abundance in the corresponding starting lysates was confirmed by immunoblotting (Lysate). $n = 6$ muscle extracts per data point. Data represent means ± SEM. Black lines indicate that intervening lanes have been spliced out.

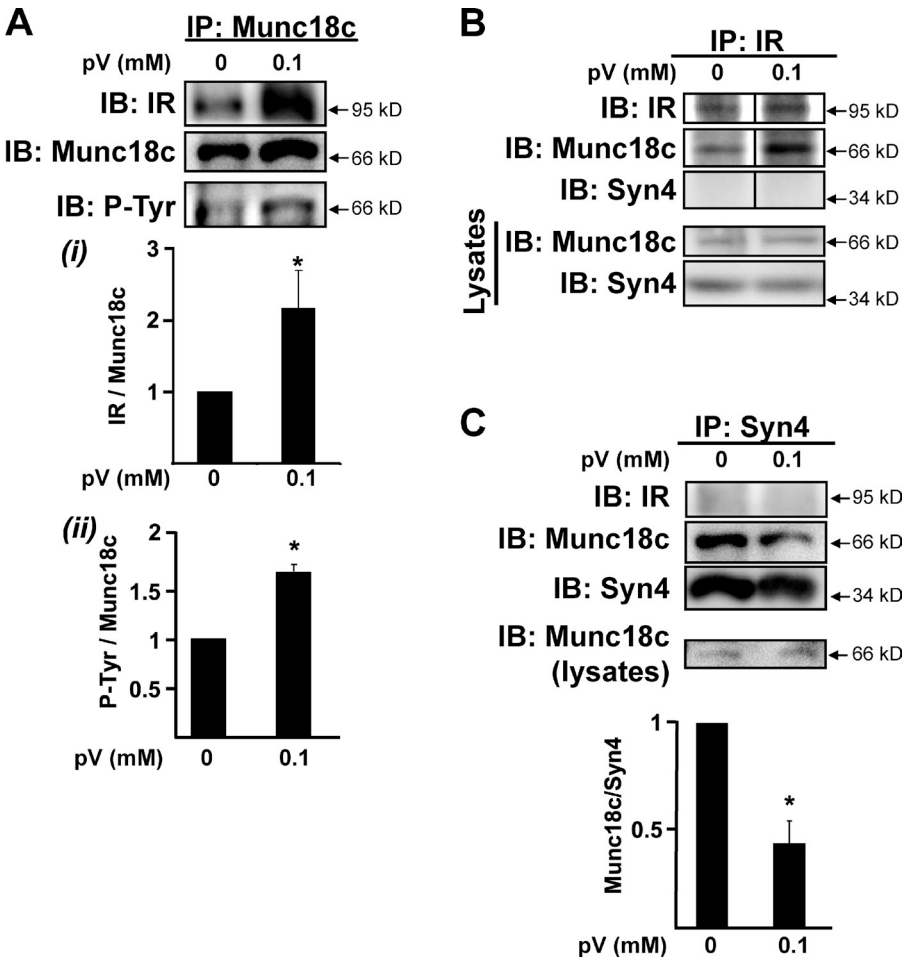

Figure 3. **pV induces IR–Munc18c complex formation and Munc18c–syntaxin 4 dissociation.** (A–C) Cleared detergent lysates prepared from fully differentiated 3T3-L1 adipocytes that were incubated in serum-free medium for 2 h and then treated with or without 0.1 mM of freshly prepared pervanadate (pV) for 5 min were used in coimmunoprecipitation (IP) reactions: anti-Munc18c (A), anti-IR (B), or anti–syntaxin 4 (C, Syn4). Anti-Munc18c and anti–syntaxin 4 immunoprecipitation reactions were processed in parallel from the same starting lysates, which were confirmed to contain equivalent Munc18c protein (lysates). Munc18c and syntaxin 4 abundances in corresponding starting lysates used for B were also confirmed (Lysates). Coimmunoprecipitated proteins were resolved on 10% SDS-PAGE for immunoblotting (IB) with anti-Munc18c, anti-IR, and anti–syntaxin 4 antibodies; the Munc18c blot was stripped and reprobed with antiphosphotyrosine 4G10 (P-Tyr). Data represent the means ± SEM from three independent experiments for each type of immunoprecipitation, quantified as the ratio of IR/total Munc18c (A, *i*), tyrosine-phosphorylated Munc18c/total Munc18c (A, *ii*), or Munc18c/total syntaxin 4 (C) immunoprecipitated, with each set normalized to untreated = 1.0; *, $P < 0.05$ versus untreated. Black lines indicate that intervening lanes have been spliced out.

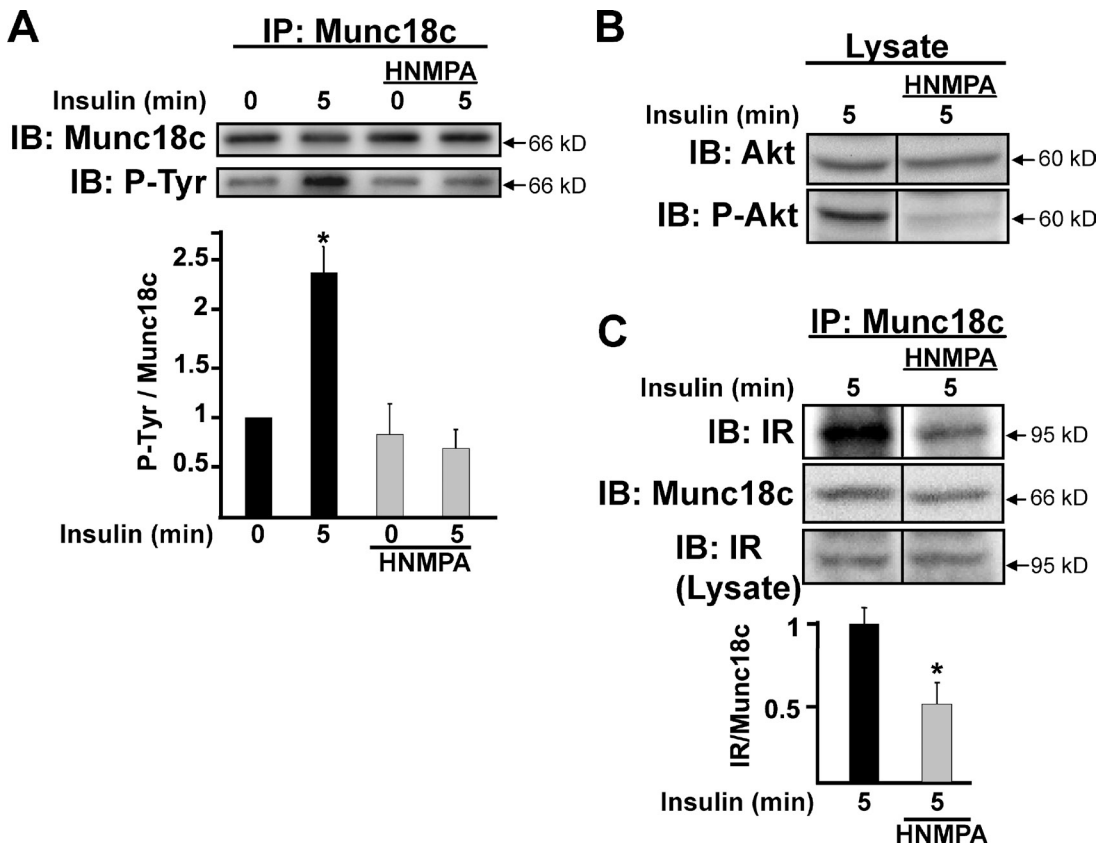

Figure 4. **IR kinase activity is required to evoke IR binding and tyrosine phosphorylation of Munc18c.** Fully differentiated 3T3-L1 adipocytes were preincubated in serum-free media for 1 h followed by an additional 1 h with or without the IR kinase activity inhibitor HNMPA-$(AM)_3$ (100 µM) before insulin stimulation for 5 min. (A) Cleared detergent lysates were prepared and used for Munc18c immunoprecipitation (IP) and detection of tyrosine-phosphorylated Munc18c (P-Tyr) using phosphotyrosine-specific 4G10 or PY20 antibodies; this experiment was performed by reprobing of the same blot with both antibodies. (B) HNMPA-$(AM)_3$ action was validated by detection of reduced Akt phosphorylation in the lysates used for immunoprecipitation; this experiment was performed by reprobing of the same blot with both antibodies. (C) IR is coimmunoprecipitated by anti-Munc18c. Coimmunoprecipitated proteins were resolved on 10% SDS-PAGE for immunoblotting (IB) with anti-Munc18c and anti-IR antibodies. IR abundance in corresponding starting lysates was confirmed by immunoblotting (Lysate). Data represent the means ± SEM from three independent sets of lysates for each panel, with each set normalized to basal = 1.0 (A) or insulin stimulation without HNMPA-$(AM)_3$ = 1.0 (C); *, $P < 0.05$ versus vehicle-treated cells. Black lines indicate that intervening lanes have been spliced out.

hydroxy-2-napthalenylmethylphosphoric acid tris-acetoxy-methyl ester (HNMPA-$(AM)_3$; Saperstein et al., 1989; Baltensperger et al., 1992) was used. Adipocytes were pretreated with 100 µM HNMPA-$(AM)_3$ for 1 h and stimulated with insulin for 5 min, and cleared detergent lysates were prepared for immunoprecipitation using the anti-Munc18c antibody. Compared with a greater than twofold increase in Munc18c tyrosine phosphorylation triggered by insulin, HNMPA-$(AM)_3$ treatment fully abolished this response to insulin (Fig. 4 A, bottom, second bar vs. fourth bar). The inhibitory action of HNMPA-$(AM)_3$ in these lysates was validated by its ablation of Akt phosphorylation (Fig. 4 B). Moreover, HNMPA-$(AM)_3$ treatment also reduced the insulin-triggered coimmunoprecipitation of IR with Munc18c to ~50% of vehicle-treated control (Fig. 4 C). These results suggested that the IR–Munc18c association and tyrosine phosphorylation of Munc18c specifically required insulin-stimulated IR kinase activity.

The tyrosine phosphorylation of Munc18c occurred within 5 min of insulin stimulation, concurrent with that of Akt activation, and Akt phosphorylation occurs downstream of PI3K activation. To determine whether the IR kinase-dependent phosphorylation of Munc18c occurred in a PI3K-dependent or -independent manner, adipocytes were pretreated with or without the PI3K-specific inhibitor wortmannin before stimulation with insulin. Interestingly, wortmannin treatment failed to reduce the level of tyrosine-phosphorylated Munc18c compared with vehicle control (Fig. 5). Wortmannin's inhibitory action in these lysates was confirmed by a decrease in Akt phosphorylation. These data suggested that the insulin-stimulated tyrosine phosphorylation of Munc18c occurred in a novel IR-dependent pathway, which was independent of PI3K/Akt activation but dependent on IR activation.

Munc18c serves as a novel IR kinase substrate in vitro

To establish the suitability of Munc18c as an IR kinase substrate, in vitro kinase assays were performed. The active IR β subunit, γ-[^{32}P]ATP, and recombinant His-tagged Munc18c protein were combined in vitro, and ^{32}P incorporation into the Munc18c protein was monitored over time by autoradiography (Fig. 6 A). In the absence of active IR, no radioactivity was incorporated, whereas its inclusion elicited a time-dependent

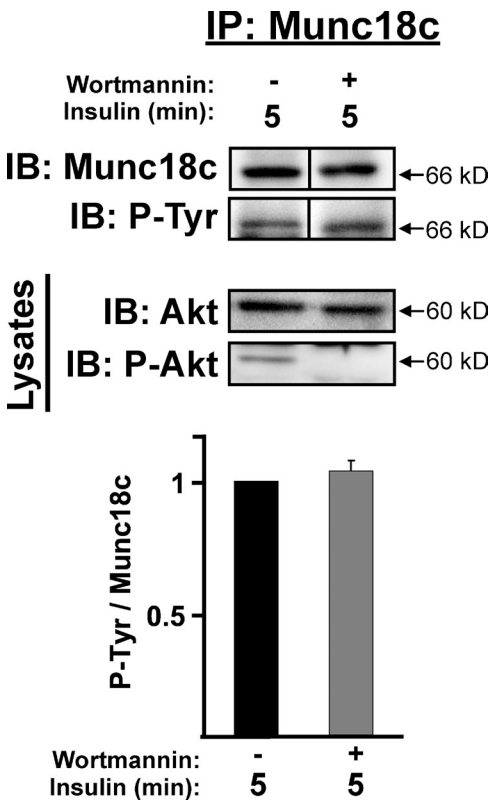

Figure 5. **Insulin stimulates the tyrosine phosphorylation of Munc18c in a PI3K-independent pathway.** Fully differentiated 3T3-L1 adipocytes were preincubated in serum-free media for 2 h with or without 100 nM wortmannin followed by 5-min insulin stimulation (100 nM) and subsequent preparation of cleared detergent cell lysates. Munc18c was immunoprecipitated (IP) from lysates, protein was resolved by 10% SDS-PAGE, and tyrosine-phosphorylated (P-Tyr) and total Munc18c was detected by immunoblotting (IB) with anti-4G10 or PY20 antibodies and anti-Munc18c, respectively; this experiment was performed by reprobing of the same blot with both antibodies. Quantitation of tyrosine-phosphorylated Munc18c/total Munc18c from at least three independent cell passages, with each experiment normalized to insulin stimulation minus wortmannin = 1.0. Insulin and wortmannin actions in lysates used for immunoprecipitation were validated by detection of phosphorylated Akt (P-Akt) content, relative to total Akt. Data represent means ± SEM. Black lines indicate that intervening lanes have been spliced out.

increase in Munc18c phosphorylation. An IRS-1 peptide (inclusive of Tyr608, a well-known substrate of the IR) was used to ensure the activity of the IR β subunit, yielding a similar time-dependent incorporation (Fig. S2).

In vitro binding assays were also used to determine whether activated IR exhibited a binding preference for Munc18c alone or for Munc18c–syntaxin 4 complexes. In vitro binding reactions containing the active IR β subunit plus GST-Munc18c alone or GST-Munc18c prebound/saturated with soluble syntaxin 4 were evaluated for the abundance of tyrosine-phosphorylated GST-Munc18c. As shown in Fig. 6 B, GST-Munc18c was equivalently phosphorylated regardless of the presence of syntaxin 4 (tyrosine-phosphorylated Munc18c/total Munc18c; Munc18c alone = 0.96 ± 0.14 arbitrary units vs. the Munc18c–syntaxin 4 complex = 1.13 ± 0.32 arbitrary units; $n = 3$; $P > 0.6$), suggesting against a preferred Munc18c substrate specificity by the IR kinase.

Mapping the tyrosine-phosphorylated sites of Munc18c

Having previously shown that Munc18c Tyr219 is a key phosphorylation site in MIN6 β cells, a phosphospecific Tyr219-Munc18c peptide antibody (p^{Y219}-Munc18c) was generated and used to detect the cellular localization of tyrosine-phosphorylated Munc18c. Consistent with the phosphotyrosine pattern of Munc18c in plasma membrane fractions of β cells (Oh and Thurmond, 2006), p^{Y219}-Munc18c–specific antibody labeling of the plasma membrane of pV-treated 3T3-L1 adipocytes was detected (Fig. 7 A, image 1). The specificity of the p^{Y219}-Munc18c antibody was verified by competition with the synthetic phosphorylated antigenic peptide, whereas competition with the same quantity of nonphosphorylated peptide was without effect (Fig. 7 A, image 3 vs. image 2). Fig. 7 A (image 4) verified the presence of adipocytes on the coverslip used to image Fig. 7 A (image 3). Fig. 7 B demonstrates the specificity of the p^{Y219}-Munc18c antibody for a pV-induced band migrating at ∼67 kD, which was consistent with phosphorylated Munc18c. Thus, these data showed the Tyr219 site within Munc18c to be a putative IR target for insulin-stimulated phosphorylation.

Munc18c residue Tyr521 was identified in a proteomic screen as an insulin-sensitive phosphorylation site (Schmelzle et al., 2006). To investigate the requirement for Munc18c Tyr219 and Tyr521 residues for modification by IR, each residue was mutated to phenylalanine and expressed as a GST fusion protein for in vitro kinase assays. GST-Munc18c-Y219F, -Y521F, or -WT proteins linked to glutathione beads were incubated with recombinant active IR β subunit and ATP, after which beads were pelleted, and proteins were resolved by SDS-PAGE for the evaluation of Munc18c phosphorylation. Consistent with the in vitro kinase assay data of Fig. 6, GST-Munc18c-WT incorporated phosphate, as detected by anti-4G10 immunoblotting (Fig. 8 A). Surprisingly, only the GST-Munc18c-Y521F mutant showed impaired phosphorylation; GST-Munc18c-Y219F phosphorylation was similar to that of WT, revealing Tyr521 to be the target of IR kinase-mediated Munc18c phosphorylation. Both Flag-Munc18c-Y219F and -Y521F proteins expressed in electroporated adipocytes coimmunoprecipitated endogenous IR, similar to Flag-Munc18c-WT (Fig. 8 B). All forms of Munc18c were equally stable as GST fusion proteins and expressed equivalently in adipocytes.

Next, we tested the ability of each mutant for association with syntaxin 4 in the absence and presence of insulin stimulation. Because overexpression of Munc18c in adipocytes reportedly deregulates normal association/dissociation patterns of Munc18c–syntaxin 4 complexes (Umahara et al., 2008), we used CHO cells stably expressing IR (CHO/IR). CHO/IR cells contain very low levels of endogenous Munc18c and transfect with high efficiency (70–90% compared with 30–50% in adipocytes), enabling the evaluation of mutant Munc18c–syntaxin 4 associations in response to insulin (Thurmond et al., 1998; Thurmond and Pessin, 2000). As previously shown, syntaxin 4 bound to Munc18c-WT under basal conditions, and this level of interaction was significantly attenuated by ∼50% in response to insulin stimulation (Fig. 8 C; Thurmond et al., 1998). However, whereas syntaxin 4 bound to the Munc18c-Y219F and -Y521F

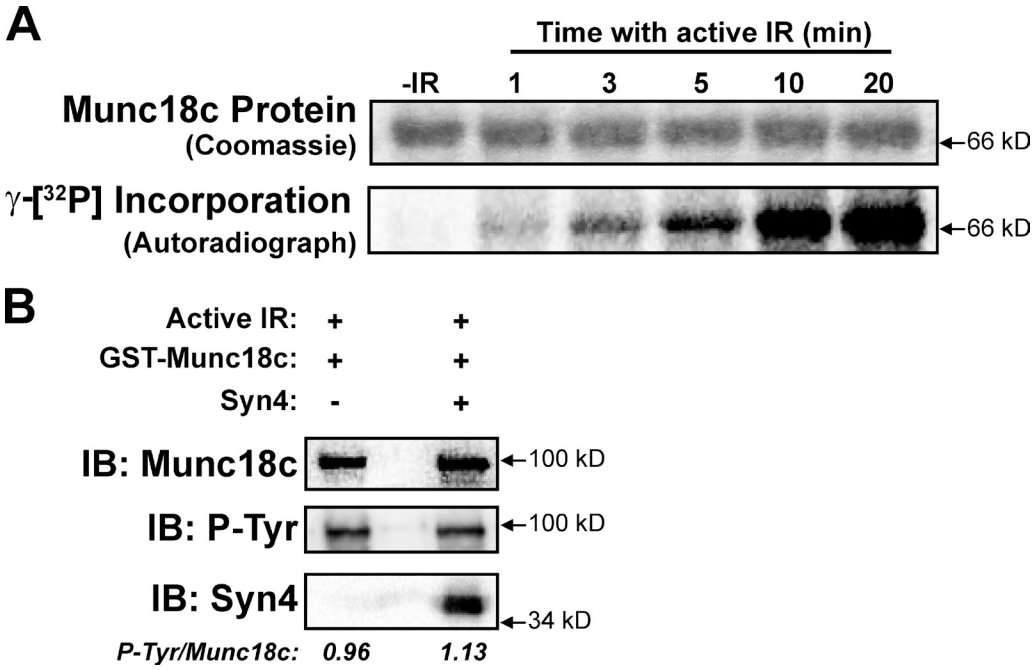

Figure 6. **Munc18c suffices as a substrate for the IR in vitro.** (A) Recombinant His-Munc18c was incubated in the presence of γ-[^{32}P]ATP with or without (−IR) the active β subunit of IR. Kinase reactions were stopped after the times indicated by the addition of SDS loading buffer. Incorporation of γ-[^{32}P]ATP into the His-Munc18c protein was detected by autoradiography. His-Munc18c input into each reaction was validated by Coomassie staining. (B) In vitro kinase reactions included active IR β subunit plus either GST-Munc18c alone or GST-Munc18c prebound by syntaxin 4 (Syn4). The mean ratio of tyrosine-phosphorylated (P-Tyr) Munc18c/total Munc18c is listed below each reaction type. All data are representative of three experiments, each using two independent batches of recombinant proteins. IB, immunoblot.

mutants under basal conditions, syntaxin 4 failed to dissociate from either in response to insulin stimulation (vs. basal = 1, insulin-stimulated ratio syntaxin 4/Flag-Munc18c-Y219F = 1.0 ± 0.1, and -Y521F = 1.6 ± 0.2). These data suggested an importance of these sites for insulin-stimulated Munc18c phosphorylation and its dissociation from syntaxin 4.

Munc18c phosphorylation at Tyr219 and Tyr521 is required for insulin-stimulated GLUT4 vesicle docking/fusion

To delineate the functional requirement for Munc18c phosphorylation at these putative sites in insulin-stimulated GLUT4 vesicle exocytosis, the endogenous Munc18c protein level was reduced via coelectroporation of 3T3-L1 adipocytes with small hairpin RNA (shRNA) plasmid (siMunc18c; Oh and Thurmond, 2009), coordinate with the coexpression of Flag-tagged Munc18c-WT, -Y219F, or -Y521F mutants (with Flag-tagged proteins made resistant to RNAi). Phosphomimetic Tyr219 and Tyr521 mutants were also examined. Coelectroporations further included the Myc-GLUT4-GFP plasmid to serve as the visible reporter of GLUT4 vesicle localization and fusion with the plasma membrane (Chen et al., 2006; Williams and Pessin, 2008).

We first sought to establish the effect of reduced endogenous Munc18c upon insulin-stimulated GLUT4 translocation in 3T3-L1 adipocytes. Because the Myc epitope is inserted into the first exofacial loop of GLUT4, it becomes externalized upon insulin-stimulated fusion of vesicles containing Myc-GLUT4-GFP with the plasma membrane, as detected by anti-Myc antibody labeling in nonpermeabilized cells (Fig. 9 A, images 1–4). The Myc tag thus distinguishes GLUT4 vesicles that are fused versus those docked with the plasma membrane. Under basal conditions, siMunc18c-expressing cells resembled control cells by demonstrating the characteristic punctate pattern of GFP (GLUT4) fluorescence in the absence of detectable Myc staining, which is consistent with a low level of fused GLUT4 in the absence of stimulation (Fig. 9 A, images 5 and 6). Insulin-stimulated GLUT4 fusion emerges as early as 5 min, requiring ∼30 min to detect a prominently outlined "rim" around the cell perimeter, at which time >80% of Myc-GLUT4-GFP–expressing cells cotransfected with control siRNA (siCon) demonstrated the Myc rim (Fig. 9 A, graph). In contrast, insulin-stimulated Myc rim formation was evident in significantly fewer cells of the siMunc18c-transfected group (Fig. 9 A, images 7 and 8 and graph). Although it was not feasible to quantify Munc18c abundance per cell by immunofluorescence because of issues related to antibody sensitivity in this application, immunoblots of lysates from siMunc18c-treated cell populations were found to contain less Munc18c protein (60 ± 6%; $P < 0.05$) relative to control (Fig. S3 A, siCon), which was consistent with thorough knockdown in a cell type known to transfect with ∼50% efficiency. Insulin-stimulated 2-deoxyglucose uptake into siMunc18c-treated adipocytes was similarly inhibited (Fig. S3 B). These results suggested a requirement for Munc18c in the insulin-stimulated GLUT4 vesicle fusion and glucose uptake of 3T3-L1 adipocytes and corroborated prior analyses performed with the skeletal muscle of Munc18c$^{+/-}$ knockout mice (Oh et al., 2005). Notably, downstream Akt activation was normal in Munc18c$^{+/-}$ muscle extracts, suggesting against a requirement for Munc18c in an upstream step of the same signaling cascade.

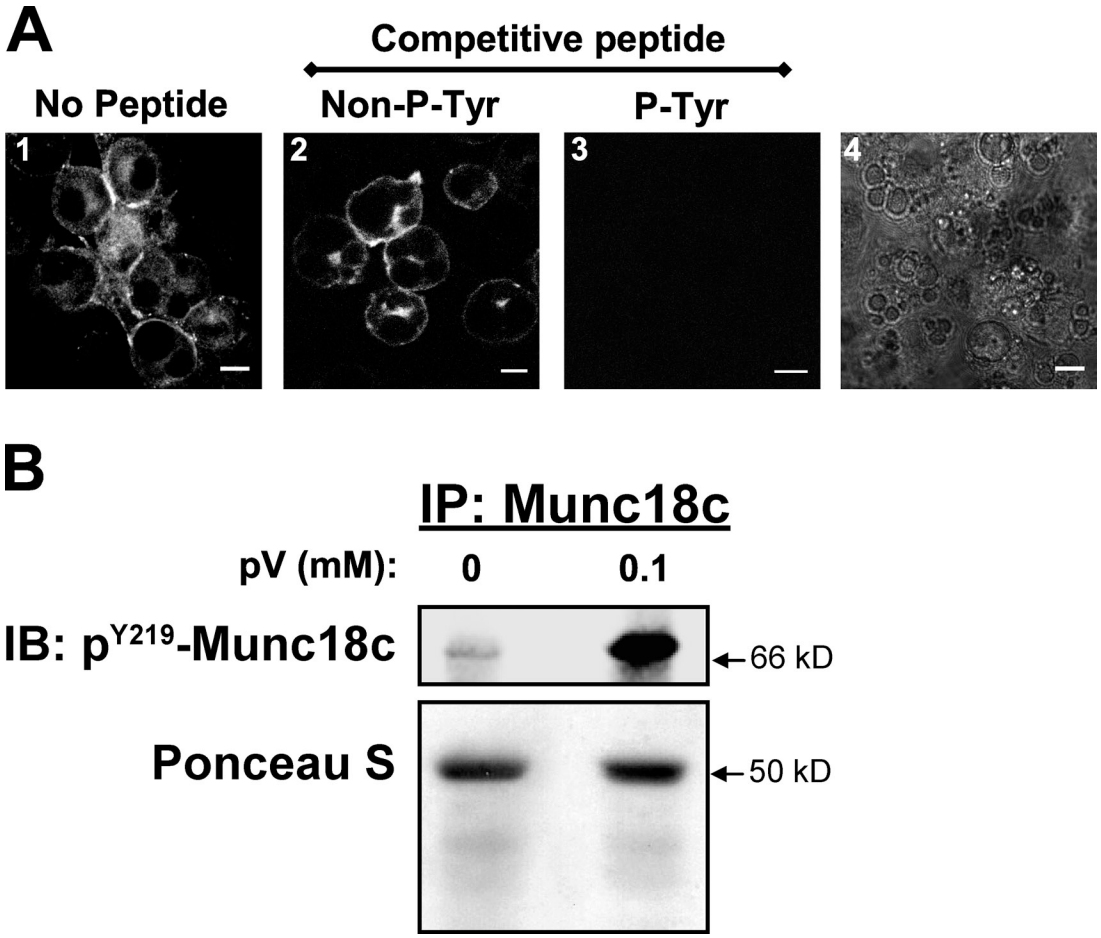

Figure 7. **Tyrosine phosphorylation of Munc18c maps to a motif centered at Tyr219 in adipocytes.** Fully differentiated 3T3-L1 adipocytes were preincubated in serum-free media for 2 h followed by treatment with freshly prepared 0.1 mM pervanadate (pV) for 5 min. (A) Cells were immediately fixed and permeabilized for immunostaining with a phosphospecific anti–p^{Y219}-Munc18c peptide antibody in the absence of a competitive peptide (image 1). The specificity of the antibody for the Y219-centered phosphopeptide was assessed by competition with the addition of 500 ng of the antigenic peptide in its nonphosphorylated (Non–P-Tyr, image 2) or phosphorylated (P-Tyr, image 3) state. Image 4 validates the presence of cells in the field imaged in image 3. Immunofluorescent confocal microscopy was used to visualize ≥50 cells each. Bars, 10 µm. (B) Cleared detergent lysates were prepared for anti-Munc18c immunoprecipitation (IP). Protein was resolved on 10% SDS-PAGE for immunoblotting (IB) with anti–p^{Y219}-Munc18c antibody. Ponceau S staining shows equal loading of the immunoprecipitation reactions. All data are representative of two to three independent experiments.

To investigate the importance of the Y219 or Y521 Munc18c phosphorylation sites, we further introduced Flag-tagged WT or mutant Munc18c plasmids into 3T3-L1 adipocytes by coelectroporation with shRNA and Myc-GLUT4-GFP reporter plasmids. GLUT4-GFP vesicle docking and/or fusion was evaluated in permeabilized cells by the presence of the GFP rim in these assays because only ∼70% of the subset of GLUT4-GFP–expressing cells exhibited clear Flag immunofluorescence. The occurrence of insulin-stimulated GLUT4-GFP rim formation and the effect of siMunc18c upon it were similar in permeabilized and nonpermeabilized adipocytes (Fig. S3 C). Recombinant Munc18c protein expression was titered to match or exceed endogenous protein expression by less than twofold to eliminate unwanted overexpression effects (Fig. S4 A). Greater than 70% of siMunc18c-treated cells coexpressing Flag-Munc18c-WT showed a restoration of insulin-stimulated GLUT4-GFP cell surface distribution compared with cells expressing vector alone (Fig. 9 B, No Flag, images 1 and 2, and graph). In contrast, expression of Flag-Munc18c-Y219F or Flag-Munc18c-Y521F (Fig. 9 B, images 3 and 4 and graph) failed to rescue insulin-stimulated GLUT4-GFP cell surface recruitment. This was not attributable to alterations of GLUT4-GFP expression in siMunc18c-treated cells (Fig. 9 A, images 1 and 5), nor did recombinant Munc18c-WT or mutant expression alter basal Myc or GLUT4-GFP localization from that of endogenous (not depicted). Importantly, expression of phosphomimetic Flag-Munc18c-Y219E, -Y521E, or a double mutant (Y219E/Y521E) resulted in the full restoration of insulin-stimulated GLUT4-GFP rim formation, similar to that of Flag-Munc18c-WT (Fig. 9 B, images 5–7). Flag expression patterns for WT and mutant forms of Munc18c were similarly cytosolic with some cell surface localization (Fig. 9 B, images 9–14), similar to the pattern of endogenous Munc18c in 3T3-L1 adipocytes. Phosphomimetic mutants displayed a capacity for binding to IR in a manner similar to Munc18c-WT (Fig. S4 B). Distinct from the Y219F and Y521F Munc18c proteins, phosphomimetic Flag-Munc18c proteins were capable of dissociating from syntaxin 4 in CHO/IR cells in an insulin-dependent manner (Fig. S4 C).

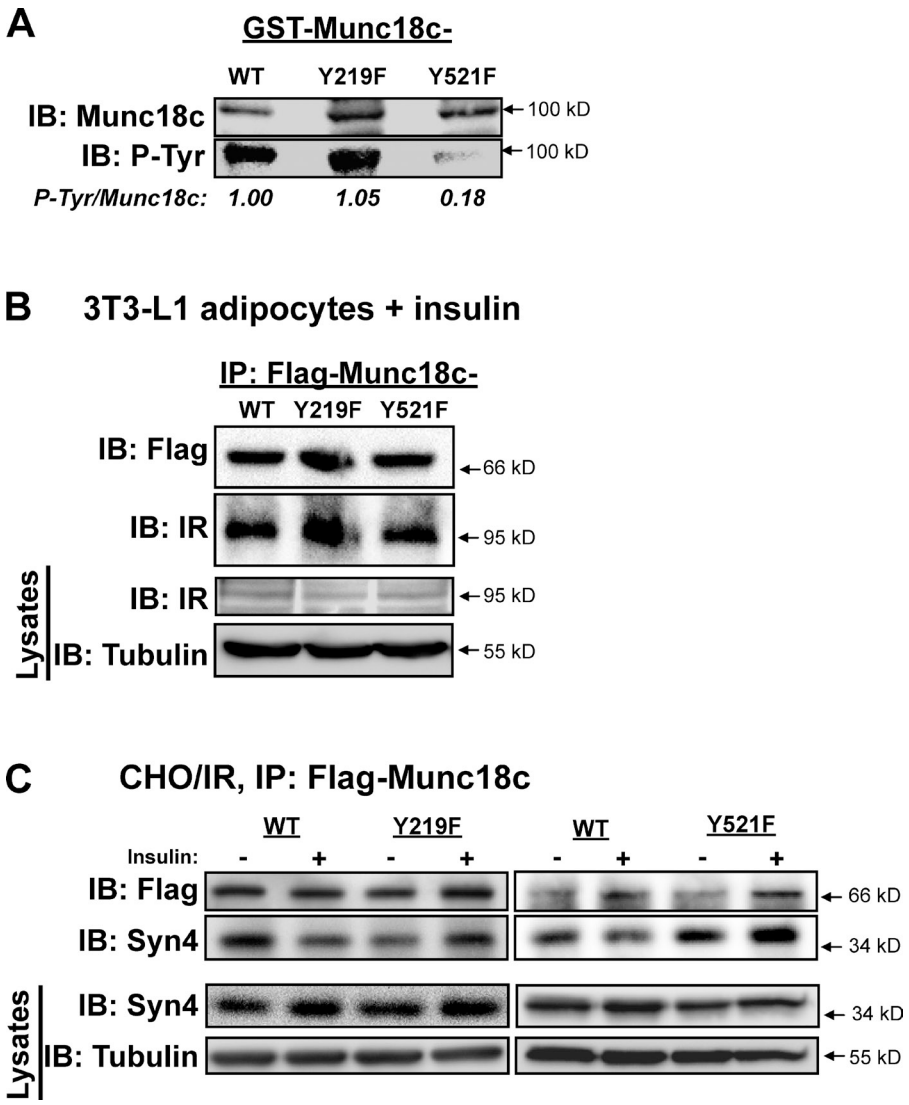

Figure 8. **IR binding and phosphorylation of Munc18c at Tyr219 and Tyr521 and the requirement for each to mediate Munc18c dissociation from syntaxin 4.** (A) Recombinantly expressed and purified GST-Munc18c-WT, GST-Munc18c-Y219F, and GST-Munc18c-Y521F proteins linked to glutathione–Sepharose beads were incubated in the presence of nonradiolabeled ATP and the active β subunit of the IR for 30 min. Reactions were stopped by the addition of Laemmli sample buffer, and GST fusion proteins were pelleted and stringently washed for resolution on 10% SDS-PAGE for the detection of phosphorylation using the antityrosine phosphorylation antibody 4G10. Expression and capture of GST fusion proteins were validated by immunoblotting (IB) for Munc18c, and data from two to three independent experiments using different protein batches were quantified as tyrosine-phosphorylated (P-Tyr) Munc18c/GST-Munc18c, normalized in each to WT = 1. (B) Electroporated adipocytes expressing Flag-Munc18c-WT, -Y219F, or -Y521F mutants were incubated in serum-free medium for 2 h and stimulated with insulin for 5 min for subsequent detergent lysis and utilization in anti-Flag immunoprecipitation (IP) reactions to detect an association with endogenous IR by immunoblotting. Equivalent IR abundance in corresponding starting lysates was confirmed on a separate gel, with tubulin as a loading control (Lysates). (C) CHO/IR cells coelectroporated to express Flag-Munc18c-WT, -Y219F, or -Y521F mutants with full-length syntaxin 4 (Syn4) were incubated in serum-free medium for 2 h and left unstimulated or were insulin stimulated for 30 min for subsequent detergent lysis and utilization in anti-Flag immunoprecipitation reactions to detect dissociation from endogenous syntaxin 4 by immunoblotting as previously described (Thurmond et al., 1998). Reactions with Y219F or Y521F, each with a paired WT-positive control, were resolved on two separate gels. Equivalent syntaxin 4 expression in corresponding starting lysates was confirmed on a separate gel, with tubulin as a loading control (Lysates). (B and C) Data are representative of at least three independent experiments using multiple DNA batches.

Therefore, regardless of their differential substrate requirements for IR-mediated phosphorylation in vitro, both Tyr521 and Tyr219 phosphorylation sites of Munc18c were required to confer its positive function in the process of insulin-stimulated GLUT4 vesicle exocytosis in 3T3-L1 adipocytes.

Discussion

In this study, our data are consistent with a functional requirement for Munc18c phosphorylation in GLUT4 vesicle exocytosis. We found that, in 3T3-L1 adipocytes and mouse skeletal muscles, insulin triggers the tyrosine phosphorylation of Munc18c concomitant with its association with the IR and disruption of Munc18c–syntaxin 4 complexes. IR kinase activity is required for these events, further implicating the IR as a novel Munc18c tyrosine kinase. In vitro kinase assays and Y^{219} phosphospecific antibody labeling point to Tyr521 and Tyr219, respectively, as target sites for modification in adipocytes. Moreover, although Tyr521 is in a disordered region, it is predicted to exist in close proximity to Tyr219, according to the Munc18c crystal structure (Fig. 10 A), suggesting that this spatial region is of particular importance in the transient and stimulus-coupled regulation of Munc18c–syntaxin 4 complexation. Importantly, our data support a model whereby insulin-stimulated phosphorylation of one or both of these tyrosine residues is required for normal insulin-stimulated GLUT4 exocytosis.

Our observations of phosphomimetic mutants of Munc18c restoring insulin-stimulated GLUT4-GFP vesicle exocytosis in the otherwise defective siMunc18c-expressing cells, which is coordinate with their ability to bind and release syntaxin 4 in a normal manner, are supportive of the concept of Munc18c functioning as a "gatekeeper," keeping syntaxin 4 inaccessible in the absence of an appropriate stimulus. This designation allows for integration of early data in which Munc18c was deemed a negative regulator because its overexpression exerted exclusively negative effects upon GLUT4 vesicle exocytosis in 3T3-L1 adipocytes, ex vivo in skeletal muscle (Khan et al., 2001) and in vivo in a Munc18c-overexpressing transgenic mouse model

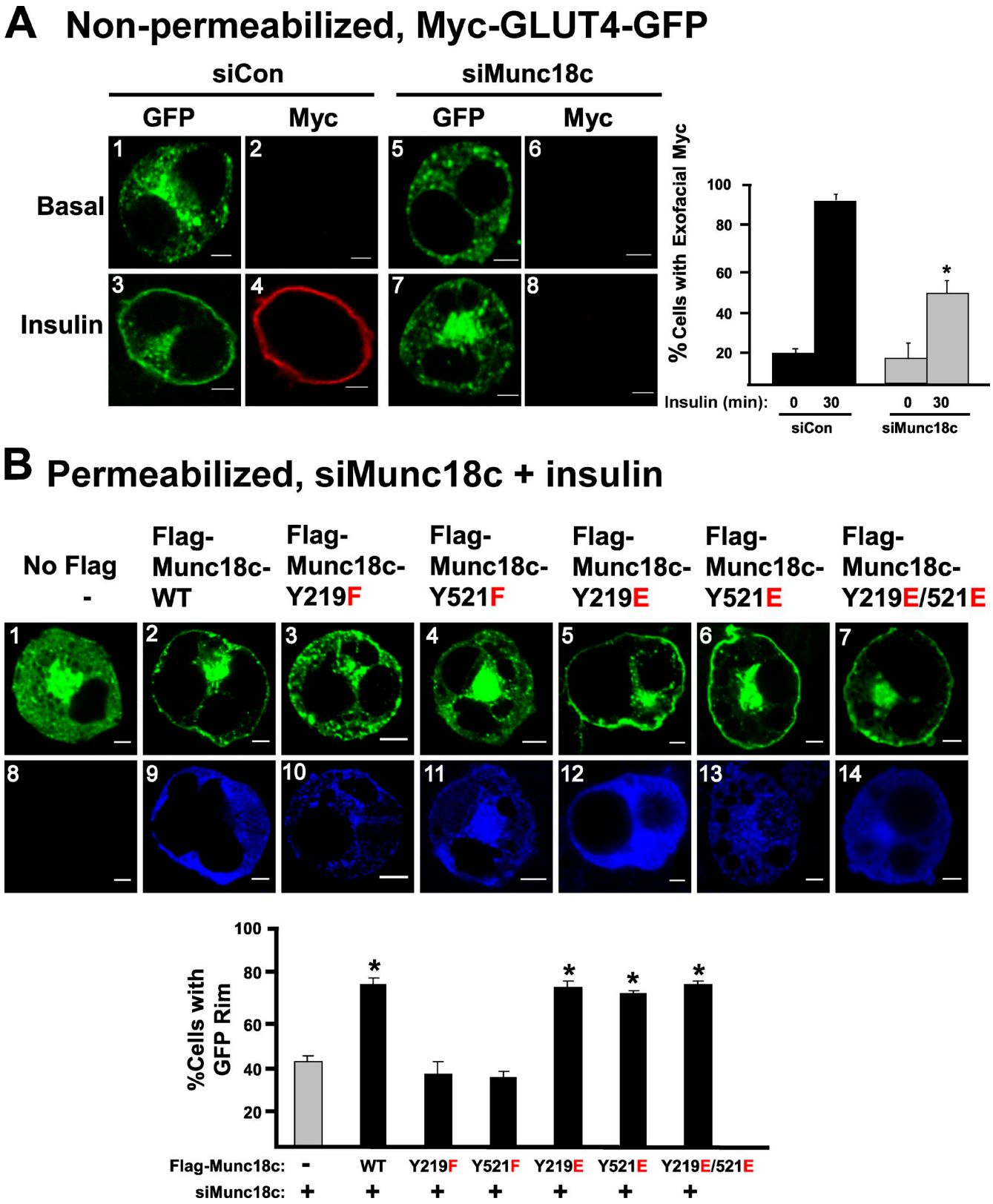

Figure 9. **Munc18c residues Tyr219 and Tyr521 are essential for insulin-stimulated GLUT4 vesicle exocytosis.** (A) 3T3-L1 adipocytes coelectroporated with Munc18c-specific (siMunc18c) or nontargeting control (siCon) shRNA plus Myc-GLUT4-GFP plasmid DNAs were left unstimulated or were stimulated with 100 nM insulin for 30 min followed by fixation but not permeabilization. Exofacial Myc exposure was determined by anti-Myc immunostaining (red) followed by immunofluorescent confocal microscopy. GFP fluorescence was examined to indicate subcellular location of GLUT4-GFP vesicles (green). The number of Myc-stained cells relative to the total number of GFP-fluorescing cells (≥50 cells per condition) was quantified in at least three independent sets of cells as depicted in the bar graph inset; *, $P < 0.05$. (B) siMunc18c shRNA and Myc-GLUT4-GFP plus either Flag-Munc18c-WT, -Y219F, -Y521F, -Y219E, -Y521E, or -Y219E/Y521E (double mutant) were coelectroporated into 3T3-L1 adipocytes as described in A and in Materials and methods and stimulated

(Spurlin et al., 2003). Moreover, this gatekeeper role is consistent with recent data from a Munc18c$^{+/-}$ mouse model (Oh et al., 2005), and RNAi experiments in islet β cells (Oh and Thurmond, 2009) have demonstrated its requirement in exocytosis, presumably by facilitating syntaxin 4–based SNARE complex formation.

Our findings that the Munc18c-Y219F and -Y521F mutants lacked the ability to dissociate from syntaxin 4 in response to the insulin stimulus, which is coordinate with the inability to restore GLUT4-GFP vesicle exocytosis in siMunc18c-expressing cells, suggested that the ability to release syntaxin 4 was functionally important. The crystal structure of Munc18c (cocrystallized with the 19 amino acid N-terminal peptide of syntaxin 4) closely resembles that of Munc18-1 in its cocrystallized conformation with soluble syntaxin 1 (Misura et al., 2000; Hu et al., 2007), which was interpreted as holding syntaxin 1 in its closed conformational state in a 1:1 stoichiometric complex. This gatekeeper-binding mode inhibits syntaxin from interacting with other SNARE proteins, presumably to halt exocytosis in the absence of appropriate stimuli. Because syntaxin 4 functions in slow exocytosis events wherein stimulus-dependent vesicle trafficking is required to initiate and sustain exocytosis, such a gatekeeper role for Munc18c to maintain syntaxin 4 in a closed and inactive form would seem logical. Very recent evidence indicates the rate-limiting step of slow exocytosis to be the stimulus-induced assembly of syntaxin–SNAP25 complexes (Takahashi et al., 2010). This concept is compatible with our prior study identifying the rate-limiting steps of GLUT4 translocation as post-IR activation or predocking (Thurmond and Pessin, 2000).

The identification of Munc18c as an IR tyrosine kinase substrate is a major step forward in understanding how insulin orchestrates GLUT4 vesicle exocytosis. Other exocytosis events involve a vesicle-associated Rab GTPase to catalyze changes in SM protein association with its syntaxin (Søgaard et al., 1994; Lupashin and Waters, 1997). Despite proteomic identification of GLUT4 vesicle Rab proteins (Larance et al., 2005; Jedrychowski et al., 2010), linkage of Rab activity specifically for Munc18c–syntaxin 4 complexes has yet to be made. It has further been hypothesized that the putative Rab for Munc18c would be activated downstream of Akt in the linear cascade emanating from IR activation (Hou and Pessin, 2007; Huang and Czech, 2007). To the contrary, our data show Munc18c phosphorylation to be wortmannin insensitive and independent of PI3K. Because IR kinase activity is required and insulin triggers phosphorylation of Munc18c within the same time frame as that of Akt activation, the existence of parallel pathways for IR-mediated Munc18c tyrosine phosphorylation and the classical IR/IRS-1/PI3K-dependent signaling cascade are supported. IR is known to use numerous substrates besides IRS-1, such as IRS proteins, Shc, Gab-1, Cbl, APS, and caveolin 1 (Kimura et al., 2002; Saltiel and Pessin, 2002), and our data indicate the necessary inclusion of Munc18c to this list of IR substrates. Insulin signaling has also been shown to bifurcate to regulate vesicle fusion and prefusion steps (Gonzalez and McGraw, 2006). This calls for a revised model whereby insulin-stimulated IR orchestrates the activation of syntaxin 4 for subsequent incoming insulin-stimulated GLUT4 vesicles in parallel to its signaling to trigger the mobilization of those vesicles. Future studies using IR knockout mice are planned to stringently test this model.

IR is the first tyrosine kinase demonstrated to bind and use Munc18c as a substrate to date. Although Umahara et al. (2008) have suggested that the PDGF receptor might serve as a kinase for residue Tyr521 of Munc18c in PDGF-stimulated GLUT4 vesicle exocytosis, they predict that the pool of Munc18c and SNARE proteins used in this process differs from those for insulin-stimulated GLUT4 vesicle translocation. However, more kinases are predicted to catalyze stimulus-specific and cell type–specific exocytosis events using Munc18c. This is predicted based upon our data showing the functional need for Tyr219 of Munc18c in insulin-stimulated GLUT4-GFP vesicle exocytosis but that IR phosphorylation of the Munc18c mutant Y219F in vitro was unimpaired. An alternate possibility is that Munc18c Tyr219 is modified in a chain of sequentially ordered phosphorylation events, requiring phosphorylation first at Tyr521. Exemplifying this, hematopoietic lineage cell-specific protein 1 (HS1) in human platelets must first be phosphorylated by Syk at Tyr397 to enable its subsequent phosphorylation by Lyn at Tyr222 (Brunati et al., 2005). This concept is further supported as Tyr521 is located within a highly disordered region, which are notable regions for posttranslational modification and induction of conformational changes (Iakoucheva et al., 2004; Collins et al., 2008; Collins, 2009), with Tyr219 predicted to be in close spatial proximity to Tyr521. Although Munc18-1 does have an analogous Tyr219, it lacks both classical and alternative upstream residues of tyrosine phosphorylation motifs, and Munc18-1 lacks Tyr521 entirely (Fig. 10 B). Similarly, Tyr219 of Munc18c only weakly matches the IR-binding motif compared with Tyr521 and may underlie the relative insensitivity of the Y219F mutant to phosphorylation by IR in vitro. In contrast, Munc18c Tyr219 is the primary site of glucose-induced phosphorylation in MIN6 β cells, although the kinase involved remains unidentified. Among other SM proteins, Tyr219 is conserved in *C. elegans* (unc18) and *Drosophila* (ROP), whereas Tyr521 is exclusive to the human and mouse Munc18c isoforms (Fig. 10 B). Altogether, the cell type and stimulus-type kinase specificity for these multiple sites provides tremendous plasticity for systems using the otherwise ubiquitously expressed Munc18c protein as a regulator of exocytosis.

If Munc18c acts as a gatekeeper, holding syntaxin 4 in a closed conformation in the absence of stimuli, the Munc18c–syntaxin 4 complex would seemingly be the preferred substrate

with insulin for 30 min. Cells were fixed and permeabilized for anti-Flag immunostaining (blue). Anti-Myc staining in permeabilized cells matched that of GFP fluorescence (not depicted). The letters in red denote the amino acid residue substitutions, with the WT form to the left and the mutant version to the right of the numbered residue in the center. In Flag-stained cells, the number of cells exhibiting a GLUT4-GFP (green) fluorescent rim around the periphery relative to the total number of Flag-GFP–fluorescing cells (≥50 cells per condition) was quantified in at least three independent sets of cells as depicted in the bar graph inset below; *, $P < 0.05$ versus cells expressing no Flag-tagged protein (vector control). Data represent means ± SEM. Bars, 5 µm.

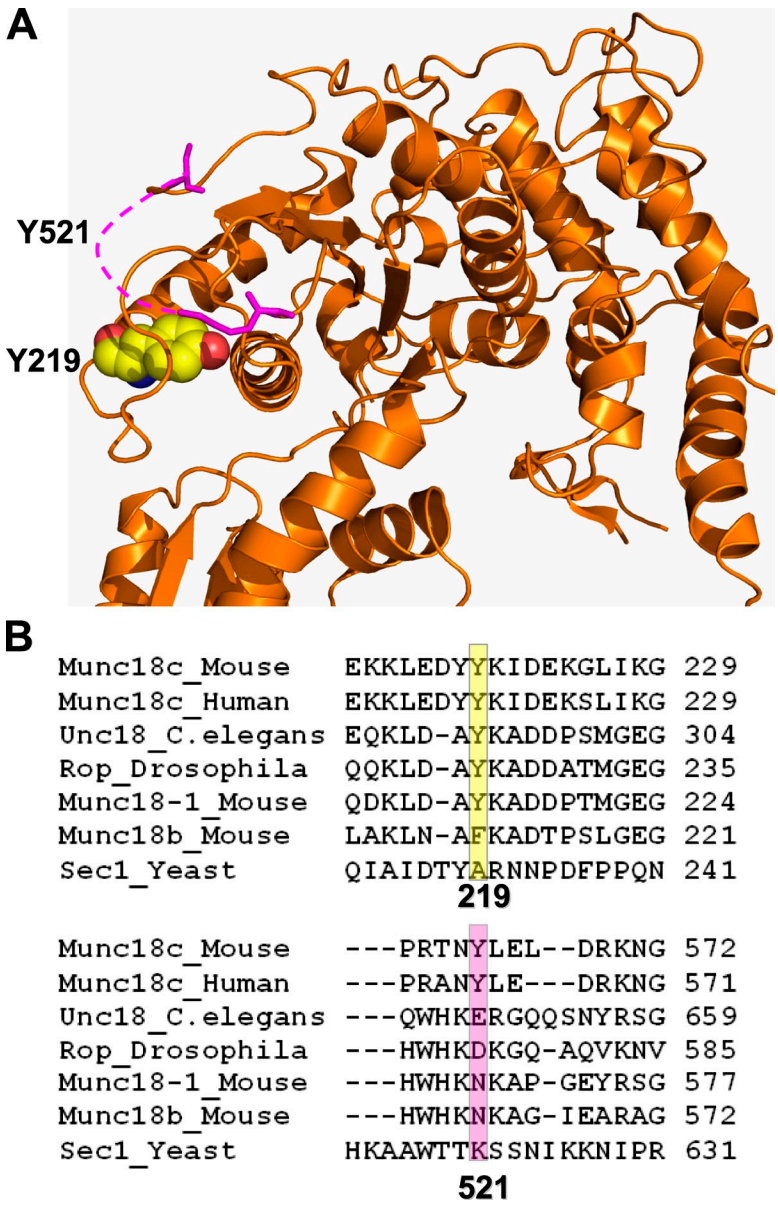

Figure 10. **Juxtaposition of Tyr219 and Tyr521 residues in the crystal structure of Munc18c and their relative conservation among SM family members.** (A) Depiction of the Munc18c (orange) crystal structure illustrating the close proximity of Tyr219 and Tyr521. The pink dashed line represents the disordered region in which Tyr521 resides. (B) ClustalW (version W2) was used to align sequences of SM proteins relative to amino acids Tyr219 and Tyr521 of mouse Munc18c. The Tyr219 site is a nonclassical NPXY motif, fitting the profile of the alternative motif with the two acidic residues at positions P4 and P3. The Tyr521 site fails to fit this alternative motif, but using NetPhosK, a kinase-specific phosphorylation site predictor (Blom et al., 2004), it is predicted as an IR kinase site. The yellow boxed region denotes the location of the amino acid residue Y219 (or amino acid otherwise) across species; the pink boxed region denotes the location of the amino acid Y521 residue (or amino acid otherwise) across species.

for IR recognition and binding compared with Munc18c alone. However, in vitro kinase assays resulted in equivalent IR-mediated phosphorylation of recombinant Munc18c whether alone or prebound by syntaxin 4. Moreover, detection of an IR–Munc18c–syntaxin 4 complex in adipocytes and skeletal muscle lysates was lacking under either unstimulated or insulin-stimulated conditions. One explanation for this could be that the dissociation of syntaxin 4 occurred immediately upon insulin-induced IR association with Munc18c, yielding undetectable amounts of syntaxin 4 in the coimmunoprecipitates. Precedence for this exists in neuronal cells, wherein the JNK-interacting protein (JIP1) associates with cognate partner dual leucine zipper kinase (DLK) under basal conditions and, upon stimulation, is joined by JNK and phosphorylated, coinciding with the dissociation of DLK from the JIP1 scaffold. DLK and JNK do not coexist simultaneously on JIP1. DLK dissociation from JIP1 results in DLK activation (Nihalani et al., 2003). Alternatively, it might also be envisioned that a signal transmitted through the N terminus of syntaxin 4 could trigger conformational changes as well, perhaps pushing Munc18c to permit IR binding and phosphorylation, generating the tyrosine-phosphorylated form of Munc18c preferentially bound by Doc2β. Doc2β facilitates insulin-stimulated GLUT4 vesicle exocytosis in 3T3-L1 adipocytes (Fukuda et al., 2009) and, in islet β cells, preferentially binds to tyrosine-phosphorylated Munc18c in a manner inversely proportional to Munc18c–syntaxin 4 binding (Jewell et al., 2008). In addition, the far N-terminal 19-mer of syntaxin 4 fits into a cleft in the Munc18c crystal structure that resides within ∼8 Å of Tyr219. Remarkably, Tyr219 maps to the minimal domain of Munc18c, which is sufficient to confer its binding to Doc2β in β cell lysates (Ke et al., 2007). Now that we recognize that Tyr521 exists in a disordered region juxtaposed to Tyr219, it will be imperative to order the interaction events surrounding that of Munc18c phosphorylation.

Diabetes and insulin resistance strongly link to Munc18c abundance in skeletal muscle and islet β cells. Because skeletal

muscle accounts for ~80% of whole-body glucose uptake, the validation of IR–Munc18c binding and phosphorylation in response to insulin in mouse muscle extracts further elevates the likelihood of these findings to be of physiological significance. Our data further elucidate why Munc18c might be required—to relay a signal from IR to the SNARE machinery. Although it is clear that IR targets Munc18c at residue Tyr521, its direct utilization of Tyr219 remains unclear, and an additional kinase may be involved. In conclusion, our data give rise to a novel model wherein a single extracellular signal, such as insulin, can elicit a coordinated response through activation of a tyrosine kinase, such as IR, to evoke t-SNARE assembly in sync with vesicle mobilization to the plasma membrane, culminating in coordinate SNARE core complex formation and vesicle fusion. From a broader cell biological perspective, by such modifications through a variety of tyrosine kinases, phosphatases, and cell-specific binding factors, the ubiquitous Munc18c and syntaxin 4 machinery can be tailored to suit the stimulus-specific response of a given cell type, in lieu of expressing novel cohorts of SNARE and SM proteins.

Materials and methods

Materials

The rabbit anti-Munc18c antibody was generated as previously described (Thurmond et al., 1998). The custom Tyr219-specific peptides (phosphorylated and unmodified) used to generate and affinity purify the rabbit polyclonal Munc18c phosphotyrosine 219 peptide antibody were synthesized by PhosphoSolutions. Rabbit anti-Myc and antiphosphotyrosine monoclonal (4G10) antibodies were obtained from Millipore. Monoclonal PY20 and clathrin antibodies were purchased from BD. Rabbit polyclonal anti-phospho-Akt (Thr-308) and Akt (pan) antibodies were purchased from Cell Signaling Technology. Rabbit polyclonal anti–syntaxin 4 and monoclonal anti–IRS-1 antibodies were obtained from Millipore. Protein G plus agarose, mouse anti-Myc, anti-IR, and anti–IR HRP antibodies were purchased from Santa Cruz Biotechnology, Inc. Goat anti–mouse and anti–rabbit HRP secondary antibodies were acquired from Bio-Rad Laboratories. The monoclonal Flag antibody, insulin, wortmannin, and bovine serum albumin were purchased from Sigma-Aldrich. ECL and SuperSignal West Femto reagents were obtained from GE Healthcare and Thermo Fisher Scientific, respectively. The IR inhibitor HNMPA-$(AM)_3$ was acquired from Enzo Life Sciences.

Plasmids

The generation of pcDNA3.1-Flag-Munc18c, pGEX4T1-Syn4 (1–273), pET28a(+)-His-Munc18c, pGEX-Munc18c, pSilencer 1.0–siControl, and pSilencer 1.0–siMunc18c #2 plasmids has been previously described (Thurmond et al., 1998; Ke et al., 2007; Oh and Thurmond, 2009). The siRNA-resistant pcDNA3-Munc18c-WT, -Y219F, -Y521F, -Y219E, -Y521E, and -Y219E/Y521E (double mutation) constructs were made using a site-directed mutagenesis kit (QuikChange II; Agilent Technologies) according to the manufacturer's protocol, and DNA sequencing was used for validation.

Cell culture, coimmunoprecipitation, and immunoblotting

Murine 3T3-L1 preadipocytes were purchased from H. Green (Harvard Medical School, Boston, MA) and used as previously described (Green and Kehinde, 1974). In brief, cells were cultured in DME that contained 25 mM glucose, 10% calf serum, 100 U/ml penicillin, 100 µg/ml streptomycin, and 292 µg/ml L-glutamine at 37°C in an 8% CO_2 atmosphere. At confluence, cells were differentiated by incubation in medium containing 25 mM glucose, 10% fetal bovine serum, 1 µg/ml insulin, 1 mM dexamethasone, and 0.5 mM isobutyl-1-methylxanthine. After 4 d, the medium was changed to DME containing 25 mM glucose and 10% fetal bovine serum as previously described (Thurmond et al., 1998; Thurmond and Pessin, 2000; Kralik et al., 2002). All experiments used fully differentiated adipocytes that were between 10 and 12 d after differentiation initiation and were incubated in serum-free medium 2 h before stimulation with 100 nM insulin. CHO cells stably expressing IR (CHO/IR) were a gift from J. Pessin (Albert Einstein College of Medicine, Bronx, NY) and cultured as previously described (Thurmond et al., 1998). Cleared detergent adipocytes or CHO/IR cell lysates were prepared by solubilization of cells in NP-40 lysis buffer (1 M Hepes, pH 7.4, 1% NP-40, 10% glycerol, 50 mM sodium fluoride, 10 mM sodium pyrophosphate, 137 mM sodium chloride, 1 mM sodium vanadate, 1 mM phenylmethylsulfonyl fluoride, 10 µg/ml aprotinin, 1 µg/ml pepstatin, and 5 µg/ml leupeptin) while rotating for 10 min at 4°C. Insoluble material was removed by microcentrifugation for 10 min at 4°C. Coimmunoprecipitation reactions contained 2–4 mg of cleared whole-cell detergent lysate with a primary antibody for 2 h at 4°C followed by a second incubation with protein G plus–agarose for 2 h. The resultant immunoprecipitates were subjected to 10 or 12% SDS-PAGE followed by transfer to polyvinylidene fluoride (PVDF) membranes for immunoblotting: Munc18c and syntaxin 4 antibodies were used at 1:5,000; IRS-1, IR, clathrin, 4G10, PY20, Flag (M2), and Akt were used at 1:1,000; p-Akt was used at 1:500. Secondary antibodies conjugated to HRP were used at 1:5,000 for visualization by ECL for detection using an imaging system (Chemi-Doc; Bio-Rad Laboratories).

For generation of skeletal muscle detergent extracts, mice were first fasted for 4 h (8 am–12 pm; male, 3–4 mo; C57BL/6J) for subsequent i.p. insulin injection (10 U/kg Humulin R; Eli Lilly); control mice were injected with a similar volume of vehicle (saline). After 5 min, mice were rapidly sacrificed, and hind-limb skeletal muscles were immediately excised and snap frozen in liquid nitrogen. Frozen tissues were subsequently pulverized under liquid nitrogen and stored at −80°C until use. All subsequent steps were performed at 4°C: frozen powdered tissue samples were homogenized in 10 vol (wt/vol) of buffer (containing 50 mM Tris-HCl, pH 7.5, 0.5 mM EDTA, 2 mM EGTA, 1% Triton X-100, 0.1 mM *N*-*p*-tosyl-L-lysine chloromethyl ketone, 2 mM benzamidine, 0.5 mM phenylmethylsulfonyl fluoride, 10 µg/ml leupeptin, and 1 mM Na_3VO_4) using a tissue tearor (Tissue-Tearor; Biospec Products, Inc.). Homogenates were then centrifuged at 3,600 *g* for 10 min, and resultant supernatants were used in anti-Munc18c immunoprecipitation reactions. In brief, 2–3 mg of skeletal muscle extract was combined with 2–3 µg anti-Munc18c antibody for 2 h at 4°C followed by incubation with protein G plus–agarose for 2 h. Beads were extensively washed using lysis buffer, and coimmunoprecipitated proteins were resolved on 10% SDS-PAGE for immunoblotting.

In vitro kinase assays

In vitro protein kinase activity assays were performed by quantifying the incorporation of ^{32}P from γ-[^{32}P]ATP into recombinantly expressed and purified His-Munc18c protein using the activated β subunit of the IR as the source of the kinase (Millipore). The reaction contained 50 mM Tris HCl, pH 7.5, 0.1 mM EGTA, 0.1 mM Na_3VO_4, 0.1% β-mercaptoethanol, 10 mM $MnCl_2$, 50 µM γ-[^{32}P]ATP with a specific radioactivity of 2,000 cpm/pmol, and 40 µg His-Munc18c protein substrate incubated for the times indicated in Fig. 6 A. Reactions were stopped by the addition of Laemmli sample buffer and boiling for 5 min. Proteins were resolved on 10% SDS-PAGE, Coomassie blue stained, and dried for detection of phospholabeled proteins by autoradiography and quantitation of ^{32}P-band incorporation by scintillation counting.

Nonradioactive in vitro kinase reactions were performed using GST-Munc18c fusion proteins with nonradiolabeled ATP with or without the recombinant activated β subunit of the IR in a reaction buffer (see previous paragraph) for 30 min. The reaction was stopped with Laemmli sample buffer and subjected to 10% SDS-PAGE followed by transfer to a PVDF membrane for immunoblotting with the phosphotyrosine-specific 4G10 antibody.

Myc-GLUT4-GFP exocytosis assays

Early differentiated adipocytes were coelectroporated (0.16 kV and 960 µF) with 50 µg Myc-GLUT4-EGFP plus 200 µg of additional plasmid DNAs using a modified method of Thurmond et al. (1998). After electroporation, the cells were allowed to adhere to glass coverslips in 35-mm tissue-culture dishes for 48 h. Cells were then washed and incubated for 2 h in serum-free medium and stimulated with 100 nM insulin for 30 min followed by fixation in 4% formaldehyde for 20 min at room temperature. Fixed cells were then washed three times with PBS, pH 7.4, and permeabilized (only in cells cotransfected with pcDNA-Flag-Munc18c DNAs) with 0.2% Triton X-100 for 15 min. Fixed and permeabilized cells were rinsed with PBS three times and blocked (1% bovine serum albumin and 5% donkey serum in PBS, pH 7.4) at 4°C overnight and then incubated with a primary antibody (1:50) for 1 h and either an Alexa Fluor 405– or Alexa Fluor 555–conjugated secondary (1:50) antibody for 1 h. The Munc18c p^{Y219} primary antibody was incubated with or without 500 ng peptide competitor in its nonphosphorylated or phosphorylated state, with an FITC-conjugated secondary

antibody for detection. All fluorescence microscopy images were recorded on the laser-scanning confocal microscope (FV1000; Olympus) based on an inverted microscope (IX81; Olympus) equipped with photomultiplier tubes with 405-, 488-, and 555-nm laser lines and a 60× 1.42 NA oil immersion objective lens using Fluoview software (FV10-ASW version 1.7; Olympus) at room temperature using Vectashield (Vector Laboratories) as a mounting medium. Images were prepared for presentation using ImageJ (National Institutes of Health) with minimal processing.

Computer modeling and statistical analysis

The three-dimensional crystal structure of the Munc18c complex (Protein Data Bank accession no. 2PJX) was used to illustrate the locations of Y219 and Y521. This was performed with the computer program PyMOL (Schrödinger). All data are expressed as means ± SEM. Data were evaluated for statistical significance using Student's *t* test.

Online supplemental material

Fig. S1 shows that the IR–Munc18c association is independent of IRS-1. Fig. S2 shows that the IR phosphorylates the IRS-1 peptide in vitro. Fig. S3 shows comparable phenotypic changes in insulin-stimulated GLUT4-GFP translocation to the plasma membrane in nonpermeabilized and permeabilized 3T3-L1 adipocytes and the effects of RNAi-mediated depletion. Fig. S4 shows Munc18c mutant expression and phosphomimetic Munc18c-binding characteristics. Online supplemental material is available at http://www.jcb.org/cgi/content/full/jcb.201007176/DC1.

We are grateful to Dr. Jeffrey Pessin for his gifts of the Myc-GLUT4-GFP plasmid and CHO/IR cells. We thank Yi-Chun Chen, Cathy Meyer, and Min-Jung Kim (Korean Food and Drug Association, Seoul, South Korea) for technical assistance with this project as well as Dr. Dean Wiseman for assistance with the molecular modeling.

This paper was supported by grants from the National Institutes of Health (DK076614 and DK067912 to D.C. Thurmond; AT001846 and DK082773 to J.S. Elmendorf) and the American Heart Association (predoctoral fellowships to J.L. Jewell, M.A. Kalwat, and V.S. Tagliabracci).

Submitted: 29 July 2010
Accepted: 3 March 2011

References

Bai, L., Y. Wang, J. Fan, Y. Chen, W. Ji, A. Qu, P. Xu, D.E. James, and T. Xu. 2007. Dissecting multiple steps of GLUT4 trafficking and identifying the sites of insulin action. *Cell Metab.* 5:47–57. doi:10.1016/j.cmet.2006.11.013

Baltensperger, K., R.E. Lewis, C.W. Woon, P. Vissavajjhala, A.H. Ross, and M.P. Czech. 1992. Catalysis of serine and tyrosine autophosphorylation by the human insulin receptor. *Proc. Natl. Acad. Sci. USA*. 89:7885–7889. doi:10.1073/pnas.89.17.7885

Bergman, B.C., M.A. Cornier, T.J. Horton, D.H. Bessesen, and R.H. Eckel. 2008. Skeletal muscle munc18c and syntaxin 4 in human obesity. *Nutr. Metab. (Lond)*. 5:21. doi:10.1186/1743-7075-5-21

Blom, N., T. Sicheritz-Pontén, R. Gupta, S. Gammeltoft, and S. Brunak. 2004. Prediction of post-translational glycosylation and phosphorylation of proteins from the amino acid sequence. *Proteomics*. 4:1633–1649. doi:10.1002/pmic.200300771

Brunati, A.M., R. Deana, A. Folda, M.L. Massimino, O. Marin, S. Ledro, L.A. Pinna, and A. Donella-Deana. 2005. Thrombin-induced tyrosine phosphorylation of HS1 in human platelets is sequentially catalyzed by Syk and Lyn tyrosine kinases and associated with the cellular migration of the protein. *J. Biol. Chem.* 280:21029–21035. doi:10.1074/jbc.M412634200

Chen, G., P. Liu, G.R. Pattar, L. Tackett, P. Bhonagiri, A.B. Strawbridge, and J.S. Elmendorf. 2006. Chromium activates glucose transporter 4 trafficking and enhances insulin-stimulated glucose transport in 3T3-L1 adipocytes via a cholesterol-dependent mechanism. *Mol. Endocrinol.* 20:857–870. doi:10.1210/me.2005-0255

Chen, X.W., D. Leto, S.H. Chiang, Q. Wang, and A.R. Saltiel. 2007. Activation of RalA is required for insulin-stimulated Glut4 trafficking to the plasma membrane via the exocyst and the motor protein Myo1c. *Dev. Cell*. 13:391–404. doi:10.1016/j.devcel.2007.07.007

Collins, M.O. 2009. Cell biology. Evolving cell signals. *Science*. 325:1635–1636. doi:10.1126/science.1180331

Collins, M.O., L. Yu, I. Campuzano, S.G. Grant, and J.S. Choudhary. 2008. Phosphoproteomic analysis of the mouse brain cytosol reveals a predominance of protein phosphorylation in regions of intrinsic sequence disorder. *Mol. Cell. Proteomics*. 7:1331–1348. doi:10.1074/mcp.M700564-MCP200

Dulubova, I., S. Sugita, S. Hill, M. Hosaka, I. Fernandez, T.C. Südhof, and J. Rizo. 1999. A conformational switch in syntaxin during exocytosis: role of munc18. *EMBO J.* 18:4372–4382. doi:10.1093/emboj/18.16.4372

Foster, L.J., and A. Klip. 2000. Mechanism and regulation of GLUT-4 vesicle fusion in muscle and fat cells. *Am. J. Physiol. Cell Physiol.* 279:C877–C890.

Fukuda, N., M. Emoto, Y. Nakamori, A. Taguchi, S. Miyamoto, S. Uraki, Y. Oka, and Y. Tanizawa. 2009. DOC2B: a novel syntaxin-4 binding protein mediating insulin-regulated GLUT4 vesicle fusion in adipocytes. *Diabetes*. 58:377–384. doi:10.2337/db08-0303

Gonzalez, E., and T.E. McGraw. 2006. Insulin signaling diverges into Akt-dependent and -independent signals to regulate the recruitment/docking and the fusion of GLUT4 vesicles to the plasma membrane. *Mol. Biol. Cell*. 17:4484–4493. doi:10.1091/mbc.E06-07-0585

Gonzalez, E., and T.E. McGraw. 2009. Insulin-modulated Akt subcellular localization determines Akt isoform-specific signaling. *Proc. Natl. Acad. Sci. USA*. 106:7004–7009. doi:10.1073/pnas.0901933106

Green, H., and O. Kehinde. 1974. Sublines of mouse 3T3 cells that accumulate lipid. *Cell*. 1:113–116. doi:10.1016/0092-8674(74)90126-3

Hou, J.C., and J.E. Pessin. 2007. Ins (endocytosis) and outs (exocytosis) of GLUT4 trafficking. *Curr. Opin. Cell Biol.* 19:466–473. doi:10.1016/j.ceb.2007.04.018

Hu, S.H., C.F. Latham, C.L. Gee, D.E. James, and J.L. Martin. 2007. Structure of the Munc18c/Syntaxin4 N-peptide complex defines universal features of the N-peptide binding mode of Sec1/Munc18 proteins. *Proc. Natl. Acad. Sci. USA*. 104:8773–8778. doi:10.1073/pnas.0701124104

Huang, S., and M.P. Czech. 2007. The GLUT4 glucose transporter. *Cell Metab.* 5:237–252. doi:10.1016/j.cmet.2007.03.006

Iakoucheva, L.M., P. Radivojac, C.J. Brown, T.R. O'Connor, J.G. Sikes, Z. Obradovic, and A.K. Dunker. 2004. The importance of intrinsic disorder for protein phosphorylation. *Nucleic Acids Res.* 32:1037–1049. doi:10.1093/nar/gkh253

Inoue, M., L. Chang, J. Hwang, S.H. Chiang, and A.R. Saltiel. 2003. The exocyst complex is required for targeting of Glut4 to the plasma membrane by insulin. *Nature*. 422:629–633. doi:10.1038/nature01533

Jedrychowski, M.P., C.A. Gartner, S.P. Gygi, L. Zhou, J. Herz, K.V. Kandror, and P.F. Pilch. 2010. Proteomic analysis of GLUT4 storage vesicles reveals LRP1 to be an important vesicle component and target of insulin signaling. *J. Biol. Chem.* 285:104–114. doi:10.1074/jbc.M109.040428

Jewell, J.L., E. Oh, S.M. Bennett, S.O. Meroueh, and D.C. Thurmond. 2008. The tyrosine phosphorylation of Munc18c induces a switch in binding specificity from syntaxin 4 to Doc2beta. *J. Biol. Chem.* 283:21734–21746. doi:10.1074/jbc.M710445200

Ke, B., E. Oh, and D.C. Thurmond. 2007. Doc2beta is a novel Munc18c-interacting partner and positive effector of syntaxin 4-mediated exocytosis. *J. Biol. Chem.* 282:21786–21797. doi:10.1074/jbc.M701661200

Keller, M.P., Y. Choi, P. Wang, D.B. Davis, M.E. Rabaglia, A.T. Oler, D.S. Stapleton, C. Argmann, K.L. Schueler, S. Edwards, et al. 2008. A gene expression network model of type 2 diabetes links cell cycle regulation in islets with diabetes susceptibility. *Genome Res.* 18:706–716. doi:10.1101/gr.074914.107

Khan, A.H., D.C. Thurmond, C. Yang, B.P. Ceresa, C.D. Sigmund, and J.E. Pessin. 2001. Munc18c regulates insulin-stimulated glut4 translocation to the transverse tubules in skeletal muscle. *J. Biol. Chem.* 276:4063–4069. doi:10.1074/jbc.M007419200

Kimura, A., S. Mora, S. Shigematsu, J.E. Pessin, and A.R. Saltiel. 2002. The insulin receptor catalyzes the tyrosine phosphorylation of caveolin-1. *J. Biol. Chem.* 277:30153–30158. doi:10.1074/jbc.M203375200

Klip, A. 2009. The many ways to regulate glucose transporter 4. *Appl. Physiol. Nutr. Metab.* 34:481–487. doi:10.1139/H09-047

Kralik, S.F., P. Liu, B.J. Leffler, and J.S. Elmendorf. 2002. Ceramide and glucosamine antagonism of alternate signaling pathways regulating insulin- and osmotic shock-induced glucose transporter 4 translocation. *Endocrinology*. 143:37–46. doi:10.1210/en.143.1.37

Larance, M., G. Ramm, J. Stöckli, E.M. van Dam, S. Winata, V. Wasinger, F. Simpson, M. Graham, J.R. Junutula, M. Guilhaus, and D.E. James. 2005. Characterization of the role of the Rab GTPase-activating protein AS160 in insulin-regulated GLUT4 trafficking. *J. Biol. Chem.* 280:37803–37813. doi:10.1074/jbc.M503897200

Lupashin, V.V., and M.G. Waters. 1997. t-SNARE activation through transient interaction with a rab-like guanosine triphosphatase. *Science*. 276:1255–1258. doi:10.1126/science.276.5316.1255

Misura, K.M., R.H. Scheller, and W.I. Weis. 2000. Three-dimensional structure of the neuronal-Sec1-syntaxin 1a complex. *Nature*. 404:355–362. doi:10.1038/35006120

Nihalani, D., H.N. Wong, and L.B. Holzman. 2003. Recruitment of JNK to JIP1 and JNK-dependent JIP1 phosphorylation regulates JNK module

dynamics and activation. *J. Biol. Chem.* 278:28694–28702. doi:10.1074/jbc.M304212200

Oh, E., and D.C. Thurmond. 2006. The stimulus-induced tyrosine phosphorylation of Munc18c facilitates vesicle exocytosis. *J. Biol. Chem.* 281:17624–17634. doi:10.1074/jbc.M601581200

Oh, E., and D.C. Thurmond. 2009. Munc18c depletion selectively impairs the sustained phase of insulin release. *Diabetes*. 58:1165–1174. doi:10.2337/db08-1059

Oh, E., B.A. Spurlin, J.E. Pessin, and D.C. Thurmond. 2005. Munc18c heterozygous knockout mice display increased susceptibility for severe glucose intolerance. *Diabetes*. 54:638–647. doi:10.2337/diabetes.54.3.638

Olson, A.L., J.B. Knight, and J.E. Pessin. 1997. Syntaxin 4, VAMP2, and/or VAMP3/cellubrevin are functional target membrane and vesicle SNAP receptors for insulin-stimulated GLUT4 translocation in adipocytes. *Mol. Cell. Biol.* 17:2425–2435.

Saltiel, A.R., and J.E. Pessin. 2002. Insulin signaling pathways in time and space. *Trends Cell Biol.* 12:65–71. doi:10.1016/S0962-8924(01)02207-3

Saperstein, R., P.P. Vicario, H.V. Strout, E. Brady, E.E. Slater, W.J. Greenlee, D.L. Ondeyka, A.A. Patchett, and D.G. Hangauer. 1989. Design of a selective insulin receptor tyrosine kinase inhibitor and its effect on glucose uptake and metabolism in intact cells. *Biochemistry*. 28:5694–5701. doi:10.1021/bi00439a053

Schmelzle, K., S. Kane, S. Gridley, G.E. Lienhard, and F.M. White. 2006. Temporal dynamics of tyrosine phosphorylation in insulin signaling. *Diabetes*. 55:2171–2179. doi:10.2337/db06-0148

Schulze, K.L., J.T. Littleton, A. Salzberg, N. Halachmi, M. Stern, Z. Lev, and H.J. Bellen. 1994. rop, a *Drosophila* homolog of yeast Sec1 and vertebrate n-Sec1/Munc-18 proteins, is a negative regulator of neurotransmitter release in vivo. *Neuron*. 13:1099–1108. doi:10.1016/0896-6273(94)90048-5

Shen, J., D.C. Tareste, F. Paumet, J.E. Rothman, and T.J. Melia. 2007. Selective activation of cognate SNAREpins by Sec1/Munc18 proteins. *Cell*. 128:183–195. doi:10.1016/j.cell.2006.12.016

Shen, J., S.S. Rathore, L. Khandan, and J.E. Rothman. 2010. SNARE bundle and syntaxin N-peptide constitute a minimal complement for Munc18-1 activation of membrane fusion. *J. Cell Biol.* 190:55–63. doi:10.1083/jcb.201003148

Søgaard, M., K. Tani, R.R. Ye, S. Geromanos, P. Tempst, T. Kirchhausen, J.E. Rothman, and T. Söllner. 1994. A rab protein is required for the assembly of SNARE complexes in the docking of transport vesicles. *Cell*. 78:937–948. doi:10.1016/0092-8674(94)90270-4

Spurlin, B.A., R.M. Thomas, A.K. Nevins, H.J. Kim, Y.J. Kim, H.L. Noh, G.I. Shulman, J.K. Kim, and D.C. Thurmond. 2003. Insulin resistance in tetracycline-repressible Munc18c transgenic mice. *Diabetes*. 52:1910–1917. doi:10.2337/diabetes.52.8.1910

Südhof, T.C., and J.E. Rothman. 2009. Membrane fusion: grappling with SNARE and SM proteins. *Science*. 323:474–477. doi:10.1126/science.1161748

Takahashi, N., H. Hatakeyama, H. Okado, J. Noguchi, M. Ohno, and H. Kasai. 2010. SNARE conformational changes that prepare vesicles for exocytosis. *Cell Metab.* 12:19–29. doi:10.1016/j.cmet.2010.05.013

Tamori, Y., M. Kawanishi, T. Niki, H. Shinoda, S. Araki, H. Okazawa, and M. Kasuga. 1998. Inhibition of insulin-induced GLUT4 translocation by Munc18c through interaction with syntaxin4 in 3T3-L1 adipocytes. *J. Biol. Chem.* 273:19740–19746. doi:10.1074/jbc.273.31.19740

Tellam, J.T., S. McIntosh, and D.E. James. 1995. Molecular identification of two novel Munc-18 isoforms expressed in non-neuronal tissues. *J. Biol. Chem.* 270:5857–5863. doi:10.1074/jbc.270.11.5857

Tellam, J.T., S.L. Macaulay, S. McIntosh, D.R. Hewish, C.W. Ward, and D.E. James. 1997. Characterization of Munc-18c and syntaxin-4 in 3T3-L1 adipocytes. Putative role in insulin-dependent movement of GLUT-4. *J. Biol. Chem.* 272:6179–6186. doi:10.1074/jbc.272.10.6179

Thurmond, D.C., and J.E. Pessin. 2000. Discrimination of GLUT4 vesicle trafficking from fusion using a temperature-sensitive Munc18c mutant. *EMBO J.* 19:3565–3575. doi:10.1093/emboj/19.14.3565

Thurmond, D.C., B.P. Ceresa, S. Okada, J.S. Elmendorf, K. Coker, and J.E. Pessin. 1998. Regulation of insulin-stimulated GLUT4 translocation by Munc18c in 3T3L1 adipocytes. *J. Biol. Chem.* 273:33876–33883. doi:10.1074/jbc.273.50.33876

Timmers, K.I., A.E. Clark, M. Omatsu-Kanbe, S.W. Whiteheart, M.K. Bennett, G.D. Holman, and S.W. Cushman. 1996. Identification of SNAP receptors in rat adipose cell membrane fractions and in SNARE complexes co-immunoprecipitated with epitope-tagged N-ethylmaleimide-sensitive fusion protein. *Biochem. J.* 320:429–436.

Toonen, R.F., K. Wierda, M.S. Sons, H. de Wit, L.N. Cornelisse, A. Brussaard, J.J. Plomp, and M. Verhage. 2006. Munc18-1 expression levels control synapse recovery by regulating readily releasable pool size. *Proc. Natl. Acad. Sci. USA*. 103:18332–18337. doi:10.1073/pnas.0608507103

Umahara, M., S. Okada, E. Yamada, T. Saito, K. Ohshima, K. Hashimoto, M. Yamada, H. Shimizu, J.E. Pessin, and M. Mori. 2008. Tyrosine phosphorylation of Munc18c regulates platelet-derived growth factor-stimulated glucose transporter 4 translocation in 3T3L1 adipocytes. *Endocrinology*. 149:40–49. doi:10.1210/en.2006-1549

Weber, T., B.V. Zemelman, J.A. McNew, B. Westermann, M. Gmachl, F. Parlati, T.H. Söllner, and J.E. Rothman. 1998. SNAREpins: minimal machinery for membrane fusion. *Cell*. 92:759–772. doi:10.1016/S0092-8674(00)81404-X

Williams, D., and J.E. Pessin. 2008. Mapping of R-SNARE function at distinct intracellular GLUT4 trafficking steps in adipocytes. *J. Cell Biol.* 180:375–387. doi:10.1083/jcb.200709108

Wu, M.N., J.T. Littleton, M.A. Bhat, A. Prokop, and H.J. Bellen. 1998. ROP, the *Drosophila* Sec1 homolog, interacts with syntaxin and regulates neurotransmitter release in a dosage-dependent manner. *EMBO J.* 17:127–139. doi:10.1093/emboj/17.1.127

Xue, Y., J. Ren, X. Gao, C. Jin, L. Wen, and X. Yao. 2008. GPS 2.0, a tool to predict kinase-specific phosphorylation sites in hierarchy. *Mol. Cell. Proteomics*. 7:1598–1608. doi:10.1074/mcp.M700574-MCP200

Yang, C., K.J. Coker, J.K. Kim, S. Mora, D.C. Thurmond, A.C. Davis, B. Yang, R.A. Williamson, G.I. Shulman, and J.E. Pessin. 2001. Syntaxin 4 heterozygous knockout mice develop muscle insulin resistance. *J. Clin. Invest.* 107:1311–1318. doi:10.1172/JCI12274

Yechoor, V.K., M.E. Patti, K. Ueki, P.G. Laustsen, R. Saccone, R. Rauniyar, and C.R. Kahn. 2004. Distinct pathways of insulin-regulated versus diabetes-regulated gene expression: an in vivo analysis in MIRKO mice. *Proc. Natl. Acad. Sci. USA*. 101:16525–16530. doi:10.1073/pnas.0407574101

Zhang, W., A. Efanov, S.N. Yang, G. Fried, S. Kolare, H. Brown, S. Zaitsev, P.O. Berggren, and B. Meister. 2000. Munc-18 associates with syntaxin and serves as a negative regulator of exocytosis in the pancreatic beta-cell. *J. Biol. Chem.* 275:41521–41527. doi:10.1074/jbc.M005479200